

Remembering forward: Neural correlates of memory and prediction in human motor adaptation

Robert A. Scheidt^{a,b,c,*}, Janice L. Zimelman^{c,d}, Nicole M.G. Salowitz^a, Aaron J. Suminski^a, Kristine M. Mosier^e, James Houk^f, Lucia Simo^f

^a Department of Biomedical Engineering, Marquette University, Milwaukee, WI, USA

^b Department of Physical Medicine and Rehabilitation, Feinberg School of Medicine, Northwestern University, Chicago, IL, USA

^c Department of Neurology, Medical College of Wisconsin, Milwaukee, WI, USA

^d Cognitive and Motor Learning Research Program, Louis Stokes Cleveland Department of Veterans Affairs Medical Center (LSCDVAMC), Cleveland, OH, USA

^e Department of Radiology, Indiana University School of Medicine, Indianapolis, IN, USA

^f Department of Physiology, Feinberg School of Medicine, Northwestern University, Chicago, IL, USA

ARTICLE INFO

Article history:

Received 29 March 2011

Revised 22 July 2011

Accepted 23 July 2011

Available online 4 August 2011

Keywords:

Functional magnetic resonance imaging (fMRI)

Motor adaptation

Feedforward control

Learning

ABSTRACT

We used functional MR imaging (fMRI), a robotic manipulandum and systems identification techniques to examine neural correlates of predictive compensation for spring-like loads during goal-directed wrist movements in neurologically-intact humans. Although load changed unpredictably from one trial to the next, subjects nevertheless used sensorimotor memories from recent movements to predict and compensate upcoming loads. Prediction enabled subjects to adapt performance so that the task was accomplished with minimum effort. Population analyses of functional images revealed a distributed, bilateral network of cortical and subcortical activity supporting predictive load compensation during visual target capture. Cortical regions – including prefrontal, parietal and hippocampal cortices – exhibited trial-by-trial fluctuations in BOLD signal consistent with the storage and recall of sensorimotor memories or “states” important for spatial working memory. Bilateral activations in associative regions of the striatum demonstrated temporal correlation with the magnitude of kinematic performance error (a signal that could drive reward-optimizing reinforcement learning and the prospective scaling of previously learned motor programs). BOLD signal correlations with load prediction were observed in the cerebellar cortex and red nuclei (consistent with the idea that these structures generate adaptive fusimotor signals facilitating cancelation of expected proprioceptive feedback, as required for conditional feedback adjustments to ongoing motor commands and feedback error learning). Analysis of single subject images revealed that predictive activity was at least as likely to be observed in more than one of these neural systems as in just one. We conclude therefore that motor adaptation is mediated by predictive compensations supported by multiple, distributed, cortical and subcortical structures.

© 2011 Elsevier Inc. All rights reserved.

Introduction

In Lewis Carroll's *Through the Looking Glass* (Carroll, 1871), the white queen remarks, “It is a poor sort of memory that only works backwards.” Indeed, if memory is to improve fitness for survival it must shape future actions to satisfy changing environmental demands. Take for example the capture and retrieval of an early-morning cup of coffee. Lifting the cup over a laptop computer requires accurate estimation of the cup's weight. Misestimating the load can have costly consequences. As the coffee level decreases, the nervous system compensates by adjusting muscular activities through a form of motor

learning known as motor adaptation (Lackner and Dizio, 1994; Shadmehr and Mussa-Ivaldi, 1994; Thoroughman and Shadmehr, 1999). Motor adaptation relies on limited memory of prior sensorimotor experiences to adjust muscle activity in anticipation of future loads (Scheidt et al., 2001) so as to minimize kinematic performance errors (Flannagan and Rao, 1995; Shadmehr and Mussa-Ivaldi, 1994) while also minimizing “effort” (Hasan, 1986; Nelson, 1983) or other costs of control (for a review see Shadmehr and Krakauer, 2008). Experimental data show that minimization of kinematic errors progresses faster than does minimization of kinetic effort in goal-directed arm movements such that overall performance is dominated by kinematic optimization (Scheidt et al., 2000). The present study exploits these observations to ask “Which brain structures contribute to the processing of recent sensorimotor memories for the prediction and compensation of future environmental loads during goal-directed movement?”

* Corresponding author at: Department of Biomedical Engineering, Olin Engineering Center, 303, P.O. Box 1881, Marquette University, Milwaukee, WI 53201-1881, USA. Fax: +1 414 288 7938.

E-mail address: scheidt@ieee.org (R.A. Scheidt).

Psychophysical studies have provided compelling evidence that motor adaptation involves compensatory responses that occur on (at least) two time scales (Lee and Schweighofer, 2009; Smith et al., 2006), and that the different adaptive processes may have distinct neural bases (Keisler and Shadmehr, 2010). In fact, three computationally distinct forms of neural plasticity have been implicated in motor learning (Houk and Wise, 1995; see Doya, 1999, 2000 and Hikosaka et al., 2002; Hikosaka et al., 2008 for reviews) and the extent to which each contributes to predictive load compensation is unknown. First, supervised learning within microzones of the cerebellum is thought to facilitate the estimation or modeling of the state of the limb and its environment (Bursztyn et al., 2006; Imamizu et al., 2000; Ito, 2000, 2005; Kawato and Gomi, 1992; Miall et al., 1993; Wolpert et al., 1995, 1998), information that can be used to predict the sensory consequences of action (Angel, 1976; Bell et al., 2008; Blakemore et al., 2001). By comparing predicted and realized sensations, deviations from expectation provide a signed error signal (i.e. one that has magnitude and direction) that can drive both corrective actions via model reference feedback control (Houk and Rymer, 1981; see also Seidler et al., 2004) and internal model updating via feedback error learning (Kawato et al., 1987; Kawato and Gomi, 1992; see also Fagg et al., 1997). Second, reinforcement learning within the basal ganglia is thought to improve selection of motor commands based on information of the current sensorimotor state, thereby maximizing rewards or minimizing costs associated with action (cf. O'Doherty et al., 2003; Haruno and Kawato, 2006; Houk et al., 2007; Jueptner et al., 1997; Schultz et al., 1997, 2000; see also Mink, 1996; Graybiel, 2005). Commonly, rewards (costs) for reinforcement learning are modeled as scalar-valued signals that are maximized (minimized) when the desired task is performed successfully (Gurney et al., 2001a, 2001b). Third, unsupervised learning within cerebral cortex is thought to construct arbitrary mappings (associative memories) that maximize information transmission between input/output pathways via Hebbian potentiation and activity-dependent synaptic decay (cf. Luecke and von der Malsburg, 2004; Sanger, 1989; see also Linsker, 1988). Unsupervised learning enables the cortex to encode the current and recent state of the limb and its environment (Andersen and Buneo, 2002; Buneo and Andersen, 2006; Gandolfo et al., 2000; Gribble and Scott, 2002; Li et al., 2001) as well as the subject's own internal state in working memory (D'Esposito et al., 1995; Fuster and Alexander, 1971; Jonides et al., 1993). This may provide a common representational basis for sensorimotor information processing within the cerebellum and basal ganglia (Houk, 2011). Are motor adaptation and the prediction of future environmental loads largely the responsibility of just one of the neural systems described above (i.e. the cerebellum, its associated pathways and their targets; Doyon et al., 2003; Kawato and Gomi, 1992; Imamizu et al., 2000, 2004; Spelstra et al., 2000; Wolpert et al., 1998), or are these important computational functions subserved by multiple distributed modules as predicted by recent models of sensorimotor learning (Grosse-Wentrup and Contreras-Vidal, 2007; Houk and Wise, 1995; Houk, 2011; see also Doyon et al., 2003, 2009; Hikosaka et al., 2002)?

Here we examined trial-by-trial adaptation to changing mechanical loads during goal-directed wrist flexion movements. We conducted a novel neuroimaging experiment that combined human motor psychophysics, functional magnetic resonance imaging (fMRI), and engineering systems analysis techniques to identify neural responses (blood oxygenation level dependent BOLD signal fluctuations) that correlate with behavioral variables relating to signed performance errors (for supervised learning), unsigned errors (for reinforcement learning) and representations of current and past states (for unsupervised learning). Importantly, our approach allows us to form *a priori* estimates of each subject's prediction of impending environmental loads (i.e. the output of an internal model of the environment) and to identify neural correlates of these predictions.

Population analysis of functional MR images and follow-on analyses of individual subject BOLD data test the hypothesis that activities in select regions of cerebral cortex, basal ganglia, and lateral cerebellum predict changes in the limb's mechanical environment. Implications for the adaptive real-time control of limb movement are then discussed. Portions of this work have been presented previously in abstract form (Salowitz et al., 2010; Zimelman et al., 2007, 2008).

Methods

Subjects

Twenty healthy volunteers participated in this study (6 female, 14 male; mean age = 29 years, range: 19 to 46 years). All subjects scored greater than 68 on the Edinburgh Handedness Inventory (strongly right-handed; Oldfield, 1971). Potential subjects were excluded from the study if they had significant neurological, psychiatric or other medical history, or were taking psychoactive medications. Additional exclusion criteria were specific to MR scanning: pregnancy, ferrous objects within the body, low visual acuity, and a history of claustrophobia. Written informed consent was obtained from each subject in accord with the Declaration of Helsinki and institutional guidelines approved by Marquette University and the Medical College of Wisconsin.

Experimental setup

Subjects rested supine within a GE Signa 3 T EXCITE MR scanner equipped with a standard quadrature head coil. We minimized head motion within the coil using foam padding. Visual stimuli were computer-generated and projected onto an opaque screen that subjects viewed using prism glasses attached to the head coil. With arms at their sides, subjects grasped the handle of an MR-compatible, single degree-of-freedom, robotic manipulandum with their right hand (Fig. 1A). For each subject, the handle's axis of rotation was aligned with that of the wrist, and the frame of the device was secured to the forearm for support. The manipulandum was mounted on an adjustable support structure fixed to the subject's waist, positioning the manipulandum comfortably while reducing motion of the subject's proximal arm segments. The manipulandum includes a pneumatic actuator that exerts computer-controlled torques about

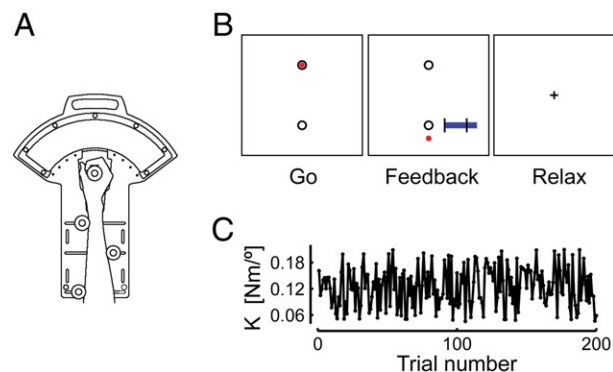


Fig. 1. (A) Schematic representation of the one-degree of freedom pneumatic manipulandum. (B) Illustration of the visual cues, summary feedback and instructions provided to subjects. Trials began with a "Go" cue wherein a black target appeared near the bottom of the screen. There was a one-to-one correspondence between the subject's actual wrist angle and the location of a red cursor on the screen. No visual feedback was provided during the movement. Instead, feedback of peak wrist angle and movement duration was presented after movement completion ("Feedback"; see Methods for details). Subjects then relaxed and visually fixated between trials ("Relax"). (C) The environmental load applied to the hand varied from trial-to-trial. For the purpose of this study, the sampling interval of behavioral data sets is 1 trial.

the wrist. Wrist position and wrist torque were monitored within 0.05° and 0.001 Nm, respectively. Analog measurements of pressure within the actuator were amplified and low-pass filtered with a cutoff frequency of 20 Hz. Joint angle measurements were also filtered at 20 Hz. Wrist angle and actuator pressure data were acquired at the control loop rate of 1000 Hz. Robot control was achieved using custom hardware and software designed to use the XPC target, real-time operating system (The Mathworks Inc., Natick, MA). Additional details of the device design, performance and MR-compatibility are described elsewhere (Suminski et al., 2007b).

Behavioral task

Subjects made 250 goal directed wrist flexion/extension movements in five blocks of 50 trials (1 movement per trial). Prior to the start of a trial, subjects were instructed to relax and visually fixate on a central crosshair stimulus while the robot held the hand at the home position of 30° wrist extension. Trials began with the appearance of a “Go” cue that consisted of a pair of black circles (1 cm dia.) representing the home position (top) and goal target (bottom) at 10° wrist extension (Fig. 1B; “Go”). A circular red cursor (0.5 cm dia.) representing the current wrist angle appeared within the home target along with the GO cue. Subjects were instructed to “Wait for the GO cue, then move out-and-back to the target in one fluid motion, reversing direction as accurately as possible within the target goal without pausing.” The cursor disappeared at movement onset such that no visual feedback of ongoing motion was provided during movement. This was done to minimize the occurrence of corrective movements in the neighborhood of the target. We provided knowledge of results (KR) of kinematic performance for 1.0 s immediately upon movement reversal to promote movement accuracy (Fig. 1B, “Feedback”). KR consisted of a static display of the red cursor at the location corresponding to the end of the flexion movement (i.e. at the angle where wrist flexion velocity fell below $10^\circ/\text{s}$) on the linear scale established by the home and goal targets. A secondary graphical element provided feedback of movement duration on a linear scale that also indicated the desired movement time (400 ± 25 ms). This information was intended to encourage consistency of movement duration across both trials and subjects. Subjects were instructed to relax after the movement. Once performance feedback had disappeared, they were to visually fixate the central cross hair while the robot maintained the hand at the start location in preparation for the next trial (Fig. 1B, “Relax”). The interval between GO cues varied randomly from 8 to 18 s, with a mean of 10 s. This variable inter-trial interval maximized the ability of the fMRI deconvolution analysis (described below) to extract hemodynamic response functions (see Toni et al., 1999).

During the trials, the robot applied resistance that increased in proportion to wrist rotation in the flexion direction (i.e. a position-dependent, “spring-like” load). The first 50 trials (the practice block) were conducted prior to functional MR imaging and were performed against a load stiffness (K) of 0.13 Nm/ $^\circ$. This was done to familiarize subjects with the temporal and spatial accuracy requirements of the task. These initial practice trials were excluded from subsequent analyses. The next four blocks (the test blocks) were performed while undergoing concurrent functional MR imaging (one block per functional imaging ‘run’). Here, the load was sampled from a uniform distribution between 0.05 and 0.21 Nm/ $^\circ$ such that K varied pseudorandomly from trial to trial about a mean value of 0.13 Nm/ $^\circ$. This mean value corresponded to information about the perturbation sequence that the subject might learn. All subjects experienced the same sequence of loads (Fig. 1C). The sequence was designed to ensure insignificant correlation between loads on consecutive trials (required by the systems identification analysis described below). The total time to complete all 250 trials was about 45 min. Subjects rested 2 to 5 min between test blocks.

MR imaging

After the initial block of practice trials and prior to functional imaging, we acquired 146 high-resolution spoiled GRASS (gradient-recalled at steady-state) axial anatomic images on each subject (TE = 3.9 ms, TR = 9.5 ms, flip angle = 12° , NEX = 1, slice thickness = 1.0 mm, FOV = 240 mm, 256×224 matrix). These images allowed localization of functional activity and spatial co-registration between subjects. Functional echo planar (EP) images were collected using a single-shot, blipped, gradient echo EP pulse sequence (TE = 25 ms, TR = 2 s, FOV = 240 mm, 64×64 matrix). Thirty-five contiguous axial 4 mm thick slices were selected in order to provide coverage of the entire brain ($3.75 \times 3.75 \times 4.00$ mm voxel size). An additional 4 images were collected at the beginning of each run to allow the fMRI signal to equilibrate and 7 more were added to the end of each run to accommodate the rise and fall of the hemodynamic response.

Behavioral data analysis

We computed four kinematic measures of task performance from the flexion phase of each movement. *Movement onset* occurred when wrist flexion velocity first exceeded $10^\circ/\text{s}$. *Flexion movement offset* occurred when wrist flexion velocity subsequently dropped below $10^\circ/\text{s}$. *Movement error*, ϵ , was defined as the angular deviation from the target at flexion movement offset. *Absolute error*, $|\epsilon|$, was defined as the absolute magnitude of the quantity $(\epsilon_i - \bar{\epsilon})$ where $\bar{\epsilon}$ was the across-trials average movement error in the last 100 trials (i.e. at steady-state). We next computed secondary performance measures including *reaction time RT* (the time delay between GO cue presentation and movement onset) and *flexion movement duration* (the time between flexion movement’s onset and offset). Movements were considered unsuccessful if they were less than half the desired extent, if movement occurred in anticipation of the GO cue ($RT < 100$ ms) or if subjects were inattentive ($RT > 800$ ms). Unsuccessful movements were excluded from further analysis.

Adaptation modeling

We constructed three behavioral time series from the four test blocks performed by each subject. These included the environmental load K_i as a function of trial number i ($1 \leq i \leq 200$), a directional or ‘signed’ kinematic error ϵ_i , and the absolute error $|\epsilon_i|$, which is uncorrelated with ϵ_i as a result of nonlinear rectification. As we will show below, K_i and ϵ_i both provide information relevant to the current state of the limb and its environment. Because $|\epsilon_i|$ is zero when performance is successful and increasingly positive otherwise, it is inversely proportional to task success regardless of whether subjects over- or under-shot the target. For the purpose of our analysis, we consider $|\epsilon_i|$ a suitable proxy for a graded reward signal that might drive reinforcement learning. Note that $|\epsilon_i|$ may be correlated with other signals of importance for reinforcement learning such as the magnitude of a prediction error (assuming subjects expect to hit the target on each trial), salience (more noticeable error, more “fast” learning; cf. Keisler and Shadmehr, 2010) and, possibly, mechanisms supporting procedural learning and/or error correction processes that are themselves dependent on the magnitude but not sign of kinematic errors.

The sequence of environmental loads was uncorrelated from one trial to the next. Therefore, history-dependent changes in performance errors could not have originated from the perturbation sequence itself but rather must have originated from the processing of sensorimotor memories within the neuromotor controller (i.e. learning). Studies of motor adaptations during goal-directed movements of the arms (Scheidt et al., 2001; Scheidt and Stoekmann, 2007; Takahashi et al., 2001), legs (Emken and Reinkensmeyer, 2005) and fingers (Liu et al., 2011) have shown that this learning is

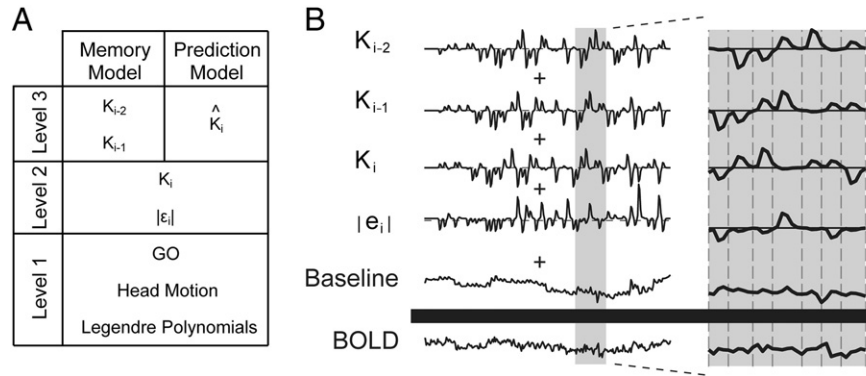


Fig. 2. Description of functional imaging analyses. (A) Two models were investigated using a sequential regression analysis comprised of three levels. Image preprocessing removed from the raw BOLD signal those signal components correlated with nuisance variables of no interest. *Level-1* analysis identified and removed from the baseline-corrected BOLD signal the general task-related activity. *Level-2* analysis identified and removed from the *Level-1* residual those signal components related to current-trial performance variables of interest. Separate *Level-3* analyses identified BOLD signal components related to memory processing and load prediction. (B) Schematic representation of the statistical model comprising our “Memory Model” analysis. Individual behavioral regressors (mean removed) were convolved with a gamma-variate function approximating the canonical hemodynamic response. These time series were scaled and summed to best fit the raw BOLD signal using multi-linear regression. The gray band (left) illustrates the expanded region (right) with “GO” cue timings shown by vertical dashed lines.

well-described by a family of limited-memory, autoregressive models with external inputs:

$$\hat{\varepsilon}_i = \sum_{m=1}^N a_m \varepsilon_{i-m} + \sum_{p=0}^Q b_p K_{i-p}, \quad [1]$$

where the a 's and b 's are constant coefficient factors scaling the influence of prior performance errors ε_{i-m} as well as current (K_i) and previous (K_{i-p}) perturbations, respectively. Constants N and Q correspond to the minimum number of memory elements needed to describe the evolution of trial-by-trial errors. The family of model structures described by Eq. (1) can represent processes having very limited memory requirements (e.g. when both N and Q are small), as well as processes having more complex dynamics.

We sought to determine the most parsimonious model structure characterizing adaptive performance changes in our wrist flexion task. We first averaged movement error across subjects on a trial-by-trial basis, thus reducing the effect of inter-subject execution variability on the structure estimation procedure. We then used the systems identification toolbox (*ident*) within the Matlab computing environment to fit all model structures of moderate complexity (N and $Q \leq 10$) to one half of the data (the estimation dataset), and evaluate the models' abilities to predict the sequence of errors in the other half (the cross-validation dataset). We used the minimum descriptor length (MDL) criterion (Ljung, 1999) to identify the structure most consistent with the information filtering manifest in the sequence of errors observed during adaptation. Of all models considered, the MDL model is the one that minimizes a modified mean-square-error (MSE) function:

$$\text{MSE}_{\text{MDL}} = \text{MSE}(1 + n \log(k) / k) \quad [2]$$

where n is the total number of parameters in the model being considered ($N+Q$) and k is the number of data points in the estimation data set. The MDL criterion offers an efficient compromise between model complexity and the quality of fit to the data. We then re-fit the resulting model to each individual subject's time series to obtain individualized estimates of model coefficients a_m and b_p .

An important observation from prior studies of adaptation to stochastic loads is that the relationship between current performance

error and magnitude of current load is often linear about the adapted load magnitude \hat{K} :

$$\hat{\varepsilon}_i = b_0 (K_i - \hat{K}) \quad [3]$$

As shown in (Scheidt et al., 2001), it is possible to obtain a trial-by-trial estimate of each subject's prediction of upcoming perturbation amplitudes, \hat{K}_i , based on the model coefficients derived from Eqs. (1) and (3) above. For example, if the adaptation model includes a single memory term for both kinematic error and environmental load (as in horizontal planar reaching; Scheidt et al., 2001; Scheidt and Stoeckmann, 2007), we obtain:

$$\hat{K}_i = -\frac{a_1}{b_0} \varepsilon_{i-1} - \frac{b_1}{b_0} K_{i-1}.$$

Likewise, if the adaptation model were to include two memory terms for load, but no memory of prior errors:

$$\hat{K}_i = -\frac{b_1}{b_0} K_{i-1} - \frac{b_2}{b_0} K_{i-2}. \quad [4]$$

Of course, subjects cannot actually predict future loads because the sequence K_j is unpredictable by design, but this in no way precludes subjects from attempting to use recent sensorimotor memories to minimize errors. \hat{K}_i is ideally suited for neuroimaging analyses of motor adaptation because it provides a trial-by-trial signature of the subject's prediction of future load based solely on memories of observable behavioral variables.

Image analysis

Functional imaging datasets were generated and analyzed using the Analysis of Functional NeuroImages (AFNI) software package (Cox, 1996). Slice values were time shifted to the midpoint of the corresponding volume using Fourier interpolation. The first 4 volumes were removed from each imaging run (test block) and the 4 imaging runs were concatenated together for each subject to yield the functional imaging datasets analyzed using sequential multilinear

regression (Draper and Smith, 1998). The rationale for this analysis is based on the fundamental geometry of least squares, which permits the partitioning of a multilinear regression into separate (sequential) regressions when the input regressors are mutually independent (orthogonal). We modeled BOLD signal fluctuations within each voxel as a combination of four independent sources of variability: a) nuisance variables (cofactors) typical of fMRI data collection; b) factors related generally to the performance of the visuomotor task (i.e. factors that do not change from one trial to the next, including the processing of visual stimuli and production of wrist flexion movements); c) factors related to how current-trial performance variables change from one trial to the next (e.g. $|\varepsilon_i|$, K_i); and d) factors identified by adaptation modeling to be related to memories of prior events (e.g. K_{i-1} , K_{i-2}), including memory-based predictions of upcoming environmental loads (e.g. \hat{K}_i). We therefore performed a sequential multilinear regression analysis wherein the unmodeled (residual) signal variations that remained after an initial *Level-1* analysis became the dependent variables to be predicted by a subsequent *Level-2* analysis. Similarly, the unmodeled signal variations that remained after the *Level-2* analysis became the dependent variables to be predicted by two subsequent *Level-3* analyses (Fig. 2A). Thus, four regression analyses were performed in total. By separating analysis of current-trial regressors from memory-related regressors, differences in the degrees of freedom inherent to the two *Level-3* models could not influence the distribution of data variance attributed to the *Level-1* and *Level-2* regressors. That is, by splitting our regression into stages or Levels, we can fairly compare the relative merits of the two *Level-3* models (see Statistical inference section below) without potential confound due to re-partitioning of variance for the earlier Level regressors, as would occur if we had instead performed separate non-sequential multilinear regressions for the memory- and prediction-model analyses (see Supplemental information online).

Baseline noise model and the Level 1 analysis: Main effect of task

We sought to eliminate from the functional image dataset those BOLD signal modulations correlated with covariate factors expected to mask signal changes of interest and to identify the task-related BOLD signal components that did not vary from one trial to the next. We considered as noise all baseline drift (modeled as the linearly-weighted set of orthogonal Legendre polynomials inclusive to order 4) as well as head motion parameters identified using an interactive, linear, least squares method for spatial registration of the image time series (AFNI program 3dvolreg; Cox, 1996). Registration yielded six scalar head motion indices per functional imaging interval (period: 1 TR): rotation about the superior–inferior S/I, anterior–posterior A/P, and left–right L/R axes along with translation along each of those axes. The across-subjects average magnitude of head rotation was $0.12^\circ \pm 0.07^\circ$ (mean ± 1 SD, here and elsewhere), $0.17^\circ \pm 0.12^\circ$ and $0.35^\circ \pm 0.28^\circ$ about the S/I, A/P, and L/R axes, respectively. Average translations were 0.34 ± 0.35 , 0.91 ± 0.28 and 0.08 ± 0.05 mm in the superior, posterior, and left directions (range: 0.03 mm and 1.51 mm); no subject was excluded from analysis due to head motion.

We considered as a main effect of the subject's task those BOLD signal fluctuations related only generally with task performance. We therefore created a trial onset time reference function using a comb function (a series of 1's and 0's) with 1's assigned to TR times of trial onset (the GO cue) and 0's assigned to the remaining imaging intervals. This time series was then convolved with a gamma variate function resembling the canonical hemodynamic response (Cohen, 1997). Note that the Legendre polynomials modeling baseline drift were fit only to functional data from TRs wherein the estimated hemodynamic response to the GO reference function fell below 1% of its maximum value, thereby removing the approximate mean of the raw BOLD signal while preserving those signal components having potential correlation with trial-by-trial fluctuations in the behavioral regressors in this and subsequent analyses.

Because the visuomotor task was persistently challenging, we expected to find robust GO-related activity in brain regions known to be engaged in visuomotor tasks, including primary and non-primary sensorimotor cortices, visual and parietal association cortices as well as regions of the cerebellum (CER), thalamus (TH) and basal ganglia (BG).

Level 2 analysis: Current-trial dependencies

The purpose of this analysis was to identify BOLD signal fluctuations that correlated significantly in time with small, trial-by-trial fluctuations in specific behavioral variables of interest (ε_i , $|\varepsilon_i|$, and K_i). Because the signed kinematic error ε_i generally demonstrates strong correlation with K_i , K_i can be interpreted as representing both environmental load and performance error, equivocally. Thus, the BOLD signal residuals resulting from the *Level-1* analysis were modeled as a linearly weighted combination of input reference functions corresponding to the state variable K_i and the absolute value of kinematic error $|\varepsilon_i|$ (representing a reinforcement reward signal). The choice to use K_i as a current-trial regressor as opposed to ε_i was further motivated by the appearance of K_i (and not ε_i) in the time series model of error we obtained from the systems identification analysis of behavioral data described below (see Eq. (6) below). As with the GO cue events, each behavioral reference function was constructed using a comb function with (typically) non-zero values assigned to TR times of trial onset and 0's assigned to the remaining imaging intervals. Unlike the GO reference function, the non-zero values were drawn sequentially from the trial-by-trial behavioral time series resulting from the kinematic analysis performed for each subject. These subject-specific reference functions were convolved with a gamma-variate function prior to multilinear regression (Fig. 2B, zoomed panel). Note that correlations between $|\varepsilon_i|$ and K_i are negligible because of the nonlinearity introduced by rectification.

Level 3 analyses: Memory and prediction models

We performed two separate *Level-3* analyses to assess the strength of neuroimaging evidence supporting the participation of the cerebellum, basal ganglia and cerebral cortices in memory-based motor adaptation. The first *Level-3* analysis (the *Memory Model Analysis*) was motivated by the results of our systems identification efforts (see Fig. 4C and Behavioral Results section): BOLD signal residuals resulting from the *Level-2* analysis were modeled as a linear combination of reference functions corresponding to memories of prior trial performance variables (K_{i-1} and K_{i-2}). The second event-related analysis (the *Prediction Model Analysis*) was motivated by Eq. (4), which was also based on the results of system identification and describes how these memories may be combined to predict upcoming environmental loads. For this analysis, we evaluated the extent to which the *Level-2* residuals correlated with \hat{K}_i . Because \hat{K}_i is a particular, subject-specific, weighted combination of K_{i-1} and K_{i-2} , the two analyses differed in the degrees of freedom available for partitioning the variability within the *Level-2* residual and therefore addressed different questions. Whereas the first assessed whether and how BOLD signal fluctuations correlated generally with trial-by-trial variations in sensorimotor memories of behavioral significance, the second analysis asked whether and how BOLD signal changes correlated with the one particular combination of sensorimotor memories that emulates trial-by-trial changes in the subject's prediction of upcoming load. In both analyses, model reference functions were convolved with a gamma-variate function prior to regression analysis. The means of all *Level-2* and *Level-3* regressors were removed prior to entering into the regression analyses to minimize the potential for spurious correlation between them and any steady-state bias missed by the noise model and *Level-1* analysis.

Statistical inference

Prior to performing multilinear regression (AFNI program 3dDeconvolve), we verified the independence of all input regressors for each subject to ensure that the analyses would be free from confound due to multicollinearity.

Subject-specific anatomical and functional images were cubically interpolated to 1 mm^3 voxels, co-registered and converted to stereotaxic coordinate space following the method of Talairach and Tournoux (Talairach and Tournoux, 1988). Functional images were blurred using a 4 mm full-width half-maximum Gaussian filter to compensate for subject-to-subject anatomical variations. For each analysis, voxel-wise t -tests were performed to compare the deconvolution fit coefficients to zero. These across-subject comparisons identified voxels with statistically significant correlation between the hemodynamic response and the input regressors. A cluster-size and thresholding technique was used to correct for multiple comparisons in the group analysis. Appropriate cluster size and individual voxel p -value thresholds were estimated by performing 10,000 iterations in a Monte-Carlo simulation using the 3dClustSim tool included within the AFNI toolkit (Cox, 1996). For the *Level-1* analysis, we used a minimum cluster size of $113\ \mu\text{l}$ and an individual voxel probability of $t = 7.407$ ($p = 1 \times 10^{-6}$) to yield a whole brain family-wise error threshold of $\alpha = 0.0001$. For the *Level-2* and *Level-3* analyses, where the regressors of interest were small trial-by-trial fluctuations in performance, this approach was unduly conservative. For these analyses, we used a lower individual voxel probability of $t = 3.950$ ($p = 0.001$) to identify regions of ‘significant’ activation (minimum cluster size of $20\ \mu\text{l}$). To further ascertain the level of confidence in our behavioral correlates, we performed a jackknife analysis ($df = 16$) repeating the population t -test analysis 18 times, each time removing a different subject from the pool. We compared the resulting clusters to the original 18-subject analysis and report the number of times each cluster dropped from significance in the jackknife analysis. We consider as high-confidence those activation regions that dropped from significance rarely (≤ 1 time) whereas low-confidence activations dropped from significance frequently (≥ 10 times).

We visualized the relationship between each regressor and the residual BOLD signals within selected, masked, brain regions of interest (ROI). We identified the centroids of the selected ROIs and warped these locations back onto each individual subject’s dataset. We then extracted a trial sequence of scalars (α_i, β_i) from each centroid voxel. The trial sequences consisted of regressor magnitude α on trial i and the raw BOLD signal β at the approximate peak of the hemodynamic response on that same trial. We then plotted the relationship between the regressor of interest and the residual BOLD signal values computed by subtracting the contributions of *all* other regressor variables, excepting the variable of interest, from the raw BOLD signal. To do so, we sorted the data pairs into five bins of equal width and ascending values of α before averaging within subjects for each bin. We then computed the across-subjects correlation coefficients between regressor magnitude and the residual BOLD signal.

Finally, for regions of overlap between the two *Level-3* models (memory and prediction), we compared the ability of each model to account for variance in the individual-subject BOLD signal using a maximum power test (Bohlin, 1978; cf. Ljung, 1999 p. 508). The null hypothesis stated that the data were generated by the model with fewest free parameters (i.e. the prediction model). The test compared the MSE computed from the residuals of each model while correcting for the difference ($d = 1$) in degrees-of-freedom between the two models. The correction factor was $k_d(\alpha)/N$ with $\alpha = 0.95$ for a χ^2 distribution $k_d(\alpha)$ with d degrees-of-freedom and N data points. Here, N was the number of trials with a full set of valid data [i.e. no unsuccessful movements for trials $i, i-1$ and $i-2$; across subjects, N averaged 177 ± 15 ; range: 144 to 195]. Data were taken from the local voxel having greatest

within-subject correlation so as to maximize the BOLD signal:noise ratio for this comparison (one datum per trial). The null hypothesis is rejected if the following holds true:

$$MSE_{pred} - MSE_{mem} \geq MSE_{mem} * \frac{1}{N} k_d(\alpha) \quad [5]$$

Error bars in figures represent ± 1 SEM.

Results

Behavioral results

As shown for a representative subject (Fig. 3), wrist angle trajectories out and back to the target were performed smoothly with an across-subject average reaction time of 490 ± 62 ms and an average flexion duration of 400 ± 18 ms. Both average values were well within their respective desired ranges. Few trials were unsuccessful (see Behavioral data analysis section in Methods), averaging only 8 ± 5 trials across subjects. Unpredictable changes in spring-like load produced considerable trial-to-trial variability in the peak extent of movement (Fig. 3 top, gray traces). However, performance was reasonably accurate on average (Fig. 3 top, black trace); this was true for all subjects. Angular velocities peaked at about $80^\circ/\text{s}$ during flexion (Fig. 3, middle). The extensor torque applied by the manipulandum varied smoothly in time (Fig. 3, bottom), in approximate proportion to wrist angle displacement. As desired, peak torque scaled linearly with commanded load (across-subject average $r^2 = 0.82$).

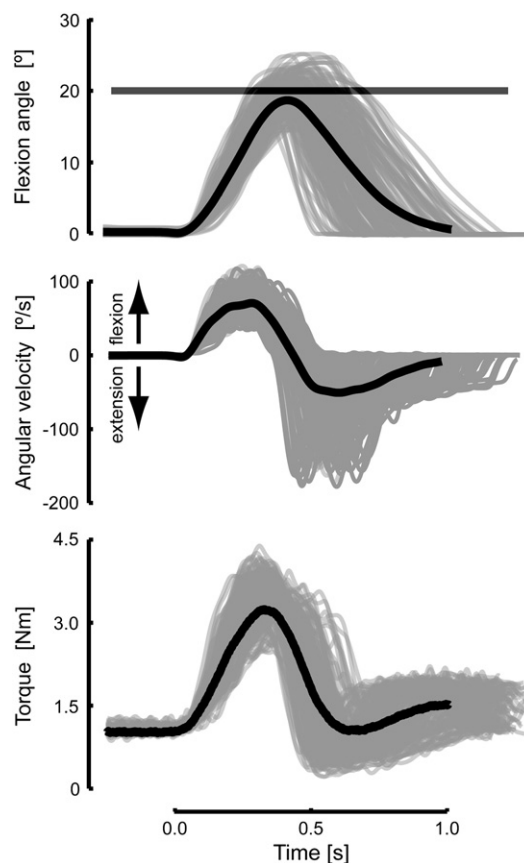


Fig. 3. Time profiles of wrist displacements (top), velocities (middle) and torques (bottom) obtained during testing of a representative subject. Individual trial profiles are presented in gray whereas the average profiles over the entire testing session are presented in black. Wrist displacement target tolerance is shown by the horizontal bar.

On average, subjects overshoot the target at the beginning of the testing session, giving rise to initial movement errors that were positively biased in the first test block (Fig. 4A, first eleven trials). This is consistent with a modest fatigue-dependent reduction in force production at the end of the baseline block, and subsequent recovery during anatomical scanning (cf. Bigland-Ritchie and Woods, 1984). If the same descending commands were applied initially after the rest as were applied before, slight overshoot would be expected at the beginning of the test blocks. We fit a falling exponential to the movement error time series, which decreased with a time constant of 31 trials (Fig. 4A, red). Asymptotic performance was approached within 100 trials; final error within the last 100 trials averaged $-0.47 \pm 2.46^\circ$ across subjects. This value closely matched the minimum movement extent (-0.50°) for which the cursor fully penetrated the target (Fig. 4A, inset). Movement errors were clearly load-dependent, varying in approximate proportion to load stiffness (Fig. 4B). When the perturbation strength was strong, the hand undershot its target whereas when the load was weak, the hand overshoot its goal. This relationship was approximately linear ($r^2 = 0.75$). The intersection of the regression line with the asymptotic error value represents the perturbation to which subjects had adapted on average ($\hat{K} = 0.129 \text{ Nm}^\circ$).

We considered whether trial-by-trial changes in kinematic error might reflect the influence of prior performance on subsequent movement attempts (cf. Scheidt et al., 2001; Scheidt and Stoeckmann, 2007; Takahashi et al., 2001). We therefore analyzed a family of linear adaptation models of moderate complexity (see Eq. (1) in Adaptation

modeling section in Methods) and found the model of Eq. (6) to be the minimum descriptor length structure (Ljung, 1999):

$$\hat{\varepsilon}_i = b_0 K_i + b_1 K_{i-1} + b_2 K_{i-2} \quad [6]$$

with 86.6% of cross-validation data variance accounted for (VAF) in the average response (Fig. 4C). While other structure selection techniques were also evaluated (including the Akaike's Information Criterion choice, AIC) (Ljung, 1999), the best improvement in data VAF over the MDL choice was 0.37% at a cost of considerable model complexity (i.e. 8 additional memory terms: 3 for perturbations and 5 for errors). Thus, Eq. (6) parsimoniously describes the average trial-by-trial changes in wrist flexion movements, demonstrating that only recent sensorimotor memories influence the updating of motor commands on subsequent trials in this task. Table 1 details the model coefficients obtained by refitting Eq. (6) to each individual subject's time series. We used these coefficients and the subject-specific behavioral time series to estimate the trial-by-trial fluctuations in each subject's prediction of the upcoming environmental load (Eq. (4)). The time series $|\varepsilon_i|$, K_i , K_{i-1} , K_{i-2} , and \hat{K}_i obtained from these analyses were used as input regressors in the sequential analysis of functional images.

Functional imaging results

To obtain reliable model coefficients, sequential regression analysis requires statistical independence of its input regressors. We

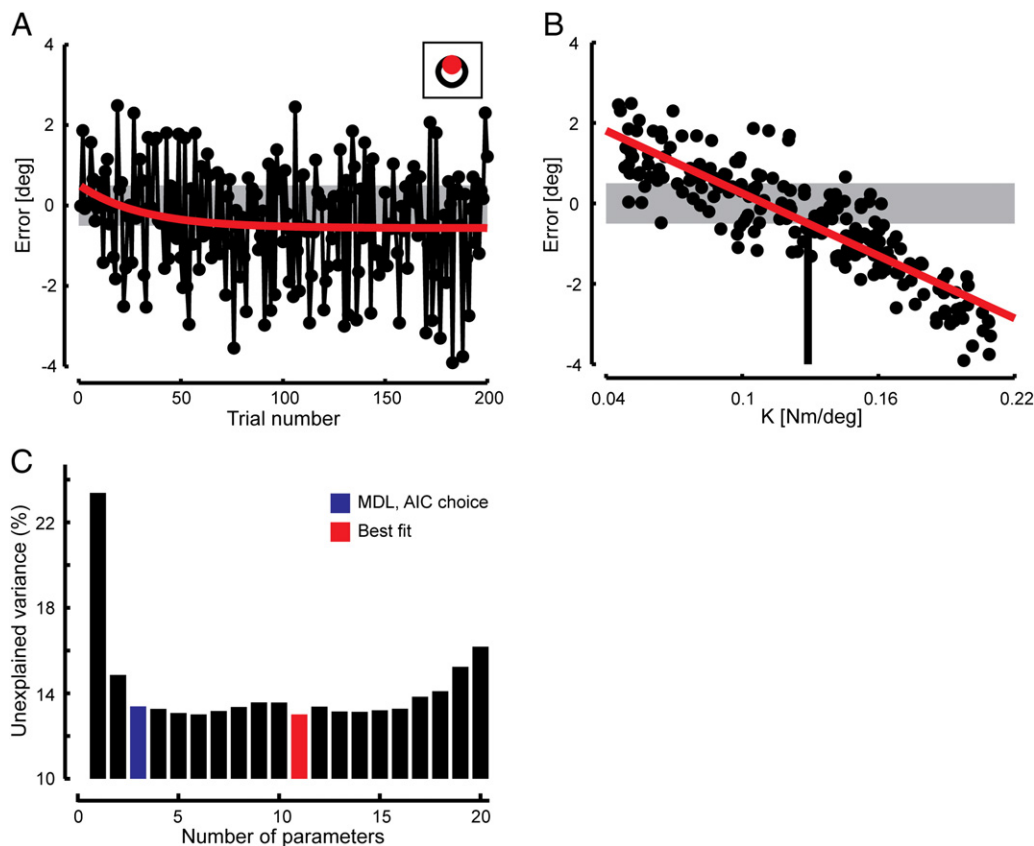


Fig. 4. Group behavioral results. (A) Time series of average movement error (black) and the line of best fit (red). Gray band indicates target tolerance. Inset shows target (black) and cursor (red) corresponding to the average subject performance at steady-state (i.e. within the last 100 trials of the experiment). (B) Average movement error plotted as a function of load stiffness on a trial-by-trial basis. The best fit linear regression is shown in red. The intersection of the regression line with the lower bound of the target tolerance indicates the mean perturbation strength that subjects had adapted to, \hat{K}_i . (C) Comparison of performance (data variance not accounted for) for models of increasing structural complexity (number of model terms, or parameters). Unexplained variance decreases dramatically with the inclusion of additional model terms up until the MDL choice model (blue) after which improvement is incremental, if at all.

Table 1
Model coefficients of behavioral time series.

Subject	b ₀	b ₁	b ₂	r ²
1	-42.7	24.1	3.5	35.2%
2	-28.4	3.9	-0.1	31.4
3	-33.0	27.1	4.4	23.0
4	-43.0	7.8	-1.6	30.5
5	-43.4	14.3	1.7	34.2
6	-32.8	4.0	9.5	28.9
7	-25.7	8.9	-1.8	16.6
8	-27.0	17.0	6.8	28.4
9	-47.5	21.2	2.4	54.6
10	-46.7	15.3	8.6	41.2
11	-28.0	5.1	10.3	14.4
12	-40.2	10.3	6.7	44.6
13 ^a	-69.0	-0.4	-4.2	47.3
14	-45.7	25.5	12.2	44.6
15	-38.8	8.1	14.6	34.6
16	-39.9	1.4	9.9	35.9
17	-26.0	5.5	8.5	14.2
18	-38.2	14.6	13.1	20.7
19 ^a	-33.7	17.7	14.7	38.2
20	-44.1	-5.8	-4.4	29.0
Mean ± SE	-39 ± 2.3	11 ± 2.0	5.7 ± 1.4	32 ± 2.5

^a Subjects excluded from image analysis due to spurious correlation between $|\epsilon_i|$ and K_i .

assessed pair-wise correlations between the behavioral regressor time series (GO, $|\epsilon_i|$, K_i , K_{i-1} , K_{i-2}) for each subject and found spurious, but statistically significant, correlations between $|\epsilon_i|$ and K_i in two subjects, who were excluded from further analysis (see Table 1).

Because \hat{K}_i is by definition a linear combination of K_{i-1} and K_{i-2} , it also was uncorrelated with the GO, $|\epsilon_i|$, K_i regressors.

Level-1 analysis – Main effect of task

We sought to identify those BOLD signal components related generally to task performance (recall that the GO signal waveform was identical on each trial). Target capture elicited widespread and distributed BOLD activation changes correlated in time with the production of goal-directed wrist movements (Fig. 5; Table 2). As expected for a right-handed visuomotor task (cf. Kawashima et al., 1995; Toni et al., 1999) requiring substantial muscle force production (Dai et al., 2001), large activation volumes spanned the central sulcus in the left hemisphere, encompassing primary sensorimotor (S1 and M1), dorsal and ventral premotor (PMd and PMv), and posterior parietal cortices (PPC). Because the subjects' target was presented visually, we expected and found widespread and distributed cortical activities in areas that contribute to visual perception, processing of visuospatial instruction cues and the encoding of visual targets relative to the initial position of the hand: middle occipital gyrus (MOG), middle temporal gyrus (MTG), fusiform gyrus (FG), lingual gyrus (LG) and anterior intraparietal sulcus/supramarginal gyrus (BA 40). Smaller cortical activation volumes were located bilaterally in cingulate, inferior parietal and insular cortices, areas thought to be involved in motor response selection in the presence of uncertainty and errors (Grinband et al., 2006; Kayser et al., 2010; Paus, 2001; Picard and Strick, 1996; Seidler et al., 2006; see also Singer et al., 2009). By construction, our task minimized the importance of online

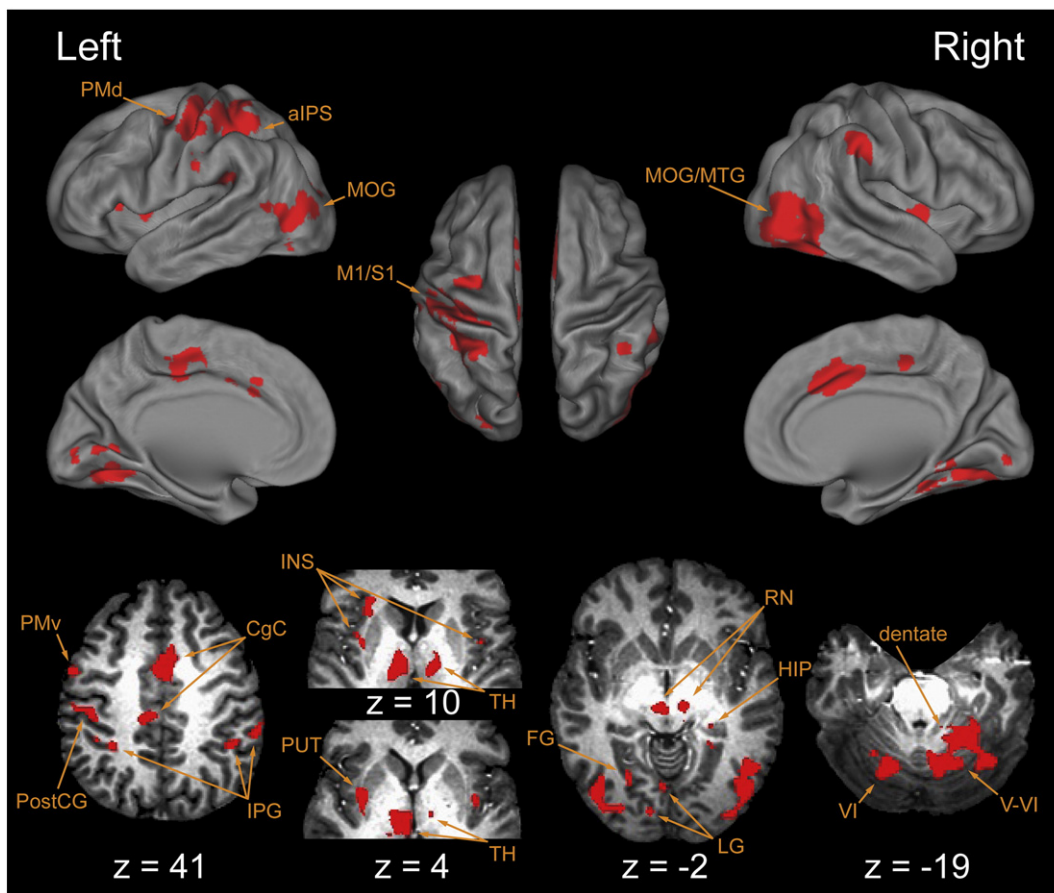


Fig. 5. Voxel-wise t-tests compared fit coefficient values versus 0.0, identifying regions that showed a statistically significant correlation between the hemodynamic response and the “GO” cue regressor. Lateral, medial and dorsal surface plots (top) and axial views (bottom) indicate cortical regions with BOLD signal components generally correlated with task execution. Here and elsewhere, left hemispheric activities are shown to the left of each panel. Abbreviations: aIPS anterior intraparietal sulcus; CgC cingulate cortex; FG fusiform gyrus; HIP hippocampus; INS insula; IPG inferior parietal gyrus; LG lingual gyrus; M1 primary motor cortex; MOG middle occipital gyrus; MTG middle temporal gyrus; PMd dorsal premotor cortex; PMv ventral premotor cortex; PostCG post central gyrus; PUT putamen; RN red nucleus; S1 primary sensory cortex; TH thalamus; V cerebellar lobule V; V1 cerebellar lobule V1.

Table 2
Location (center of mass) and volume of activations related to Level-1 Go cue.

Anatomy label	H	Vol μl	Coord			T
			x	y	z	
Cortical						
PreCG (BA 6) (PMd)	L	209	-32	-10	51	11.8
(PMv)	L	324	-52	1	38	10.8
PostCG (BA3); SPL (BA5,7); PreCG (BA4)	L	4349	-40	-26	52	15.1
SPL (BA 5,7) (IPS)	L	2405	-31	-46	50	11.6
IPL (BA 39, 40)	R	1309	54	-37	40	12.7
	L	227	-52	-19	27	9.8
	R	832	-45	-33	23	13.5
CgC (BA 32, 24); SFG (BA 6)	R/L	2421	3	6	40	13.2
pCgC (BA 31, 23); SFG (BA 6)	L/R	1255	-5	-25	45	12.0
aINS	L	587	-27	18	12	11.8
pINS	L [‡]	1163	-34	-3	10	16.9
	R	241	39	-5	4	11.5
HIP	R	165	23	-34	3	9.2
MTG (BA 37)	L	120	-45	-57	7	9.1
MOG (BA 19); LG (BA 18); FG (BA 20)	L*	8084	-30	-69	-5	14.2
MOG (BA 19); MTG (BA 37); FG (BA 20)	R [†]	15,328	31	-61	-11	13.7
LG (BA 18)	L	181	-2	-68	0	9.8
	L/R	144	-4	-83	-4	8.9
Subcortical						
pPUT; claustrum	L			<i>see[‡]</i>		
TH(VL, DM, LP), RN	L	2654	-8	-20	6	11.0
	R	323	10	-20	-1	8.9
TH(VL, DM, LP)	R	624	14	-17	12	9.8
CER(lob VI)	L			<i>see[*]</i>		
CER(lob V, VI); dentate; vermis(IV, V, VI, VIII)	R			<i>see[†]</i>		

^{*}, [†], [‡] indicates activities that extend between cortical and subcortical regions.

Abbreviations: H Hemisphere; L left; R right; Vol Volume; Coord Coordinates; T peak T; BA Brodmann's area; a anterior; p posterior; lob lobule; CER cerebellum; CgC cingulate cortex; DM dorsomedial nucleus; FG fusiform gyrus; HIP hippocampus; IPL inferior parietal lobule; IPS intraparietal sulcus; INS insula; LG lingual gyrus; LP lateral posterior nucleus; MOG middle occipital gyrus; MTG middle temporal gyrus; PMd dorsal premotor cortex; PMv ventral premotor cortex; PostCG post-central gyrus; PreCG pre-central gyrus; PUT putamen; RN red nucleus; SFG superior frontal gyrus; SPL superior parietal lobule; TH thalamus; VL ventrolateral nucleus.

feedback stabilization of wrist posture because the ballistic motions emphasized spatial accuracy at mid-movement. Nevertheless, trans-cortical feedback mechanisms probably were active during the initial "ballistic" phase of the reach (Grafton et al., 2008; Prablanc and Martin, 1992; Seidler et al., 2004; see also Desmurget et al., 1999, 2001). Consistent with so-called long-loop reflex actions (Evarts and Fromm, 1981; Evarts and Tanji, 1976; Miall et al., 1993; Strick, 1978), we observed general task-dependent activations (Fig. 5) in cortical and subcortical areas previously implicated in the closed-loop feedback compensation for limb positional errors during wrist postural stabilization (Suminski et al., 2007a, their Fig. 6) and movement (Diedrichsen et al., 2005; Grafton et al., 2008; Seidler et al., 2004). These included subcortical activations spanning anterior (lobule V) and posterior (lobule VI) regions of right lateral cerebellar cortex, deep cerebellar nuclei (interposed and/or dentate), bilateral red nucleus and bilateral activations in the cingulate motor areas that extended into the superior frontal gyri: left supra-adjacent supplementary motor area (SMA), and right pre-SMA.

Although the task was persistently novel, subjects did optimize performance by adapting to the approximate mean of the load distribution (Fig. 4B) and thus, we expected BOLD activation in areas previously implicated in the feedforward compensation for altered kinematic or kinetic behavior of a hand-held tool (Grafton et al., 2008; Imamizu et al., 2000, 2004; Jueptner et al., 1997; Krakauer et al., 2004; Seidler et al., 2004, 2006; Shadmehr and Holcomb, 1997; see also Desmurget et al., 2004). Indeed, the primary-, pre-, supplementary- and cingulate-motor area activities highlighted above could reflect these areas' contributions to motor learning (cf. Sanes, 2003). The observed activity in lobule VI of the left posterior cerebellum was in an area frequently implicated in visuospatial motor learning (Imamizu et al., 2003, their Fig. 4; Krakauer et al., 2004; Diedrichsen et al., 2005; see also Boyd and Winstein, 2004; Gilbert and Thach, 1977). Additional subcortical activations were observed in motor regions of the left striatum (posterior putamen) and bilateral thalamic nuclei: ventrolateral (VL), dorsomedial (DM) and lateralposterior (LP), structures thought to be part of cortico-thalamo-striatal-cortical

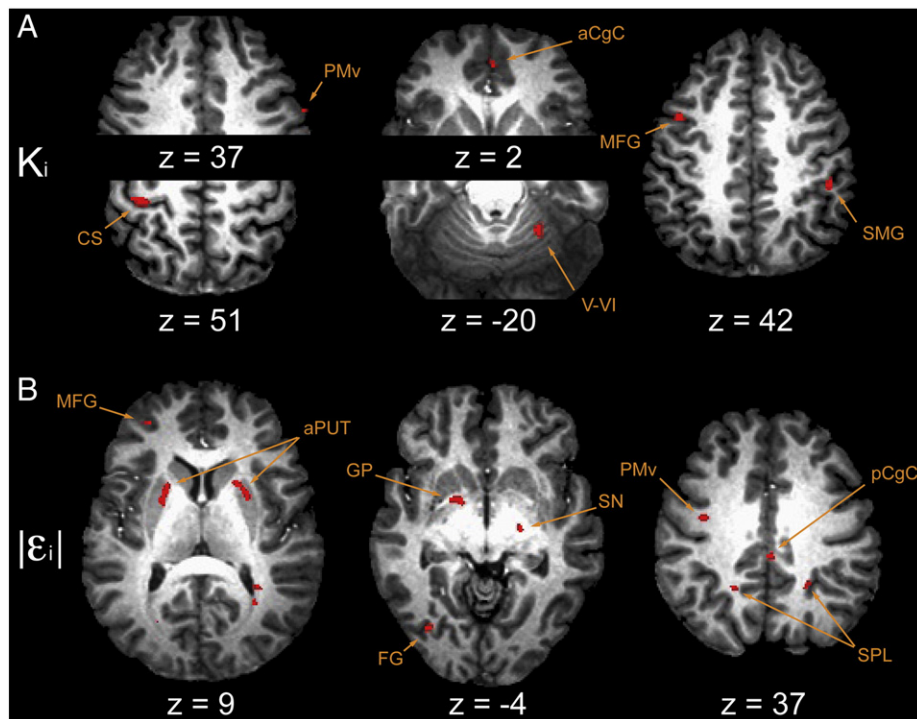


Fig. 6. FMRI results: current state regressors. (A) K_i , current trial perturbation amplitude and (B) $|\varepsilon_i|$ current trial absolute value of error. See Table 2. Abbreviations: aCgC anterior cingulate cortex; aPUT anterior putamen; CS central sulcus, pre/post central gyrus; FG fusiform gyrus; GP globus pallidus; MFG middle frontal gyrus; pCgC posterior cingulate cortex; PMv ventral premotor cortex; SMG supramarginal gyrus; SN substantia nigra; SPL superior parietal lobule; V-VI cerebellar lobule V, VI.

Table 3
Location (center of mass) and volume of activations related to Level-2 and Level-3 terms.

Anatomy label	e ₁			K _i			K _{i-1}			K _{i-2}			K̂			
	H	Vol	T	H	Vol	T	H	Vol	T	H	Vol	T	H	Vol	T	
		μl	x y z		μl	x y z		μl	x y z		μl	x y z		μl	x y z	
Cortical																
SFG (BA 6) (pre-SMA)	R [†]	21	31 8 52 4.3	L [†]	69	-41 5 42 4.9	R [†]	121	46 2 49 5.6	R	51 6 9 62 4.3	R [†]	21	7 -1 68 4.6		
MFG (BA 6) (pre-PMd)	L [†]	44	-32 37 19 4.9	L [†]	78	35 -16 65 4.8	R [†]	41	69 -20 -3 5.7	R [†]	67 51 1 47 5.1	R [†]	126	44 1 49 5.5		
MFG (BA 9,46,10) (prefrontal Ctx)	L	55	-32 45 10 4.4	R [†]	26	59 -1 37 4.2	R	38	38 -42 -18 4.8	L [†]	65 -26 32 21 4.9					
IFG (BA 44)	L [†]	52	-37 -9 37 5.7	L [†]	372	-37 -28 50 5.2	R [†]	87	16 42 6 5.4	R [†]	49 36 16 16 4.7					
PreCG (BA 6) (PMd)	L [†]	24	-27 -7 35 4.3	R	67	5 -50 34 4.6										
PreCG (BA 6) (PMv)	R [†]	40	54 -9 32 5.4	L [†]	80	-18 -50 40 5.0										
PreCG, CS, PostCG, (BA3,4)	R	49	19 -59 40 5.3	R [†]	49	19 -59 40 5.3										
Precuneus (BA 7)	R [†]	126	23 -47 37 4.8	R [†]	126	23 -47 37 4.8										
SPL	L [†]	67	5 -50 34 4.6	R [†]	57	46 -34 42 4.5										
IPS (BA7)	L	44	-49 -63 30 4.5	R [†]	22	64 -30 5 4.5										
AG (BA 39)	L [†]	23	-51 -62 26 4.5	R	22	36 -58 -9 4.5										
SMG (BA 40)	R [†]	22	64 -30 5 4.5	R [†]	58	-32 -72 -4 6.7										
STG (BA 21)	R	22	36 -58 -9 4.5	R [†]	22	2 34 29 4.4										
MTG (BA 21)	R [†]	335	16 23 29 6.7	R [†]	27	7 46 6 4.4										
MTC (BA 37)	R	27	7 46 6 4.4	R [†]	31	3 47 1 4.7										
FG (BA 20,37)	R	37	2 -31 38 4.8	R	22	36 -58 -9 4.5										
FG (BA 19)	L [†]	26	-13 -24 29 4.6	R	22	36 -58 -9 4.5										
aGgC (BA 32)	R [†]	53	5 -25 23 4.4	R	22	36 -58 -9 4.5										
pGgC (BA 23)	R [†]	23	8 -34 21 5.1	R	22	36 -58 -9 4.5										
IST	L	36	-24 -67 11 5.1	R	22	36 -58 -9 4.5										
SP	L [†]	58	-32 -72 -4 6.7	R	22	36 -58 -9 4.5										
PHIP (BA 36)	R [†]	22	2 34 29 4.4	R	22	36 -58 -9 4.5										
HIP	R [†]	335	16 23 29 6.7	R	22	36 -58 -9 4.5										
Subcortical																
aPUT	L [†]	332	-20 5 10 4.7	R	22	36 -58 -9 4.5										
GP	R [†]	229	24 8 8 4.5	R	22	36 -58 -9 4.5										
SN	L [†]	179	-16 5 -2 5.1	R	22	36 -58 -9 4.5										
TH (CM)	R [†]	39	20 -15 -4 5.9	R	22	36 -58 -9 4.5										
RN	R [†]	39	20 -15 -4 5.9	R	22	36 -58 -9 4.5										
CER (lob V, VI)	R [†]	182	25 -47 -19 4.5	R	22	36 -58 -9 4.5										
CER (lob VIII, IX)	R [†]	136	4 -40 -36 4.8	R	22	36 -58 -9 4.5										
CER vermis (lob VI–VII)	R [†]	136	4 -40 -36 4.8	R	22	36 -58 -9 4.5										
PMjd	R [†]	136	4 -40 -36 4.8	R	22	36 -58 -9 4.5										

Bootstrap results; †: **high confidence** (dropped 0–1 times); ‡: **lower confidence** (dropped 10–14 times). No region dropped 15 or more times from significance. Abbreviations: H Hemisphere; L left; R right; Vol Volume; Coord Talairach coordinates; T peak T; BA Brodmann's Area; a anterior; p posterior; lob lobule; Ctx cortex; AG angular gyrus; CER cerebellum; CgC cingulate cortex; CM centromedian nucleus; CS central sulcus; FG fusiform gyrus; GP globus pallidus; HIP hippocampus; IFG inferior frontal gyrus; IST isthmus; IPS intraparietal sulcus; MFG middle temporal gyrus; MTC middle temporal gyrus; PHIP parahippocampal gyrus; PMd dorsal premotor cortex; PMv ventral premotor cortex; PMJ ponto-medullary junction; PostCG post-central gyrus; PreCG pre-central gyrus; PUT putamen; RN red nucleus; SFG superior frontal gyrus; SMA supplementary motor area; SMG supramarginal gyrus; SN substantia nigra; SP septum; SPL superior parietal lobule; STG superior temporal gyrus; TH thalamus. ^a Indicates activities that extend between cortical and subcortical regions.

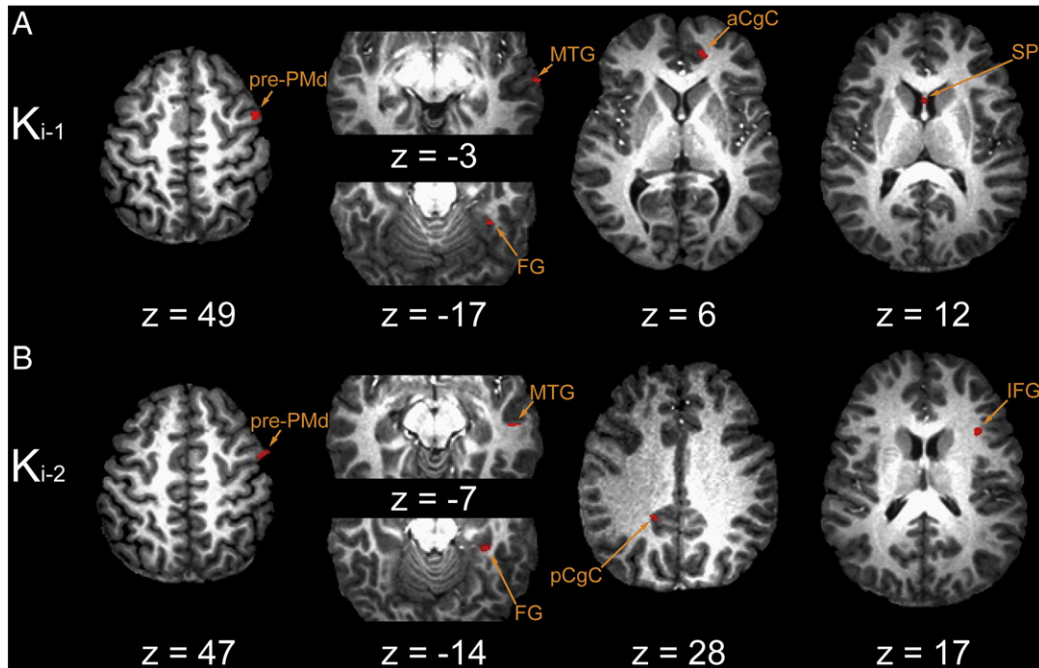


Fig. 7. FMRI results: regions with BOLD signal changes correlated with memory model terms: (A) K_{i-1} and (B) K_{i-2} . Abbreviations: aCgC anterior cingulate cortex; FG fusiform gyrus; IFG inferior frontal gyrus; MTG middle temporal gyrus; pCgC posterior cingulate cortex; PMd dorsal premotor cortex; SP septal area.

loops important for procedural and motor skill learning (Doyon et al., 2003; Graybiel, 1995; Houk, 2011; Houk and Wise, 1995; see also Seidler et al., 2006). Smaller cortical activation volumes were located in the right hippocampal/parahippocampal region, areas thought to be important for the formation and maintenance of sensorimotor and spatial memory (Burgess et al., 2002; Fuster, 2009; Nadel, 1991; Rolls, 1991, 1999) as well as other functions supporting sensorimotor integration and learning (see Bland and Oddie, 2001; Cohen and Eichenbaum, 1991; Dypvik and Bland, 2004).

Level-2 and Level-3 analyses

The sequential *Level-2* and *Level-3* analyses were intended to identify small signal modulations superimposed on the average task-related activity removed by the *Level-1* analysis. Based on Eq. (6), we hypothesized that the *Level-1* residual BOLD time series would reflect trial-by-trial fluctuations in environmental load and kinematic performance (*Level-2*) as well as fluctuations related to memories of prior loads and performances (*Level-3*).

Altogether, the *Level-2* and *Level-3* analyses revealed robust activity in multiple areas previously implicated in processing motor performance errors and the acquisition of compensatory responses reducing such errors (Table 3) (Desmurget et al., 1999; Doyon et al., 2009; Graybiel, 2005; Hikosaka et al., 1999, 2000; Imamizu et al.,

2003; Jueptner and Weiller, 1998; Miall et al., 2001; Seidler et al., 2006; Tunik et al., 2005). Confidence in the activity within each region was further assessed by a post-hoc jackknife analysis (Table 3), which counted the number of times a region dropped from significance when each subject, in turn, was excluded from analysis. Note that many regions with “small” activation volumes (<50 μ l) were robust against dropout in the jackknife analysis.

Level-2 analysis identified two large clusters of activation correlated with trial-by-trial fluctuations in K_i (Fig. 6A): left sensorimotor cortex and right cerebellar hemisphere lobule V/VI. Smaller clusters were identified in areas previously implicated in the spatial planning and execution of visually-directed movements (Boussaoud, 2001; Dieber et al., 1998; Taira et al., 1990; see also Paus, 2001): left pre-PMd, right PMd and PMv, anterior cingulate and inferior parietal cortices. BOLD signal changes in the basal ganglia correlated with trial-to-trial fluctuations in unsigned errors $|\epsilon_i|$ (Fig. 6B): bilateral anterior dorsal putamen (rostral to the anterior commissure), left globus pallidus and right substantia nigra. These areas are thought to support reinforcement learning and the conditional selection of spatially-directed motor actions and sequences of actions (Graybiel, 1998; Graybiel and Kimura, 1995; Gurney et al., 2001a, 2001b). We also found $|\epsilon_i|$ -correlated activities distributed throughout neocortical areas with reciprocal connections

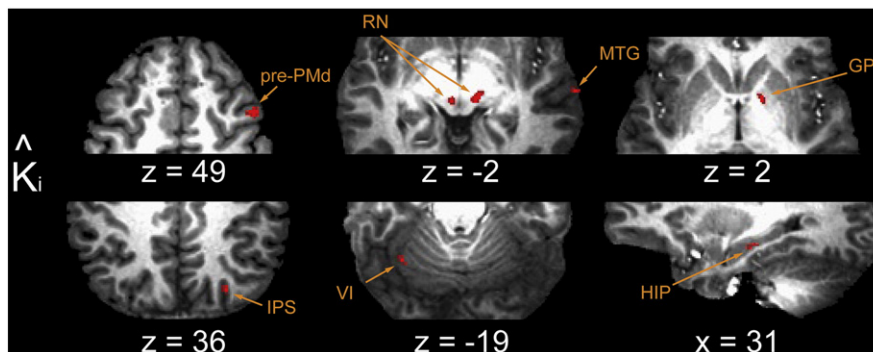


Fig. 8. FMRI results: regions with BOLD signal changes correlated with prediction model term \hat{K}_i . Abbreviations: GP globus pallidus; HIP hippocampus; IPS intraparietal sulcus; MTG middle temporal gyrus; PMd dorsal premotor cortex; RN red nucleus; VI cerebellar lobule VI.

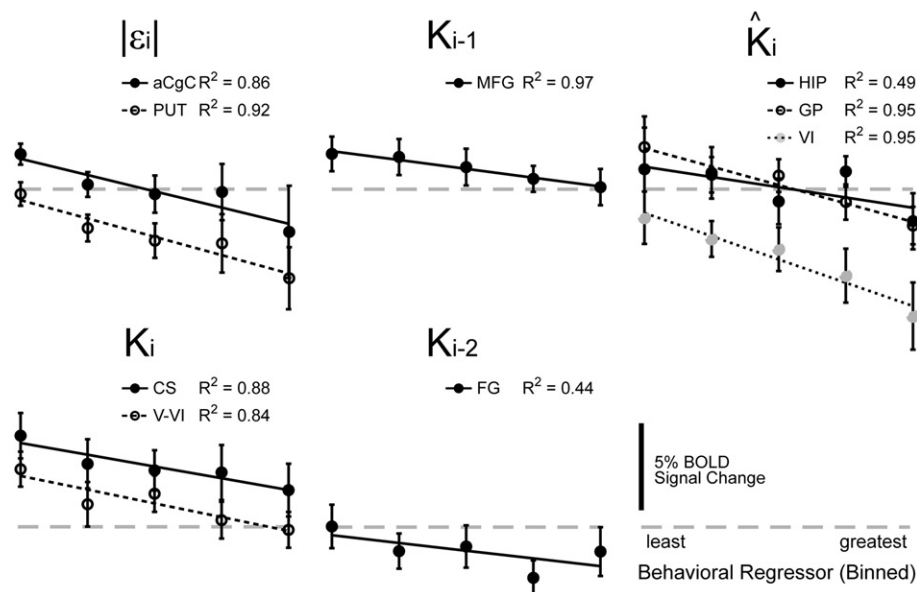


Fig. 9. BOLD activity versus binned parameter magnitude, averaged across subjects. Vertical error bars: ± 1 SEM.

to the basal ganglia (Alexander et al., 1986; Middleton and Strick, 2001; see also Selemon and Goldman-Rakic, 1985, 1988): left hemispheric pre-frontal (BA 10) and inferior parietal (BA 39) cortices; right hemispheric pre-PMd (per the convention of Picard and Strick, 2001), anterior cingulate, superior parietal and superior temporal cortices; bilateral activity in PMv, posterior cingulate, fusiform and precuneate cortices. We also found $|\varepsilon_i|$ -correlated activity within the pontomedullary tegmentum, an area that includes the inferior olive, serotonergic raphe nuclei and reticulospinal projections.

Both of the Level-3 analyses modeled the Level-2 residuals as a weighted combination of prior trial perturbation K_{i-1} and K_{i-2} reference waveforms. In the *memory model* analysis (Fig. 7), the regression treated the memories independently and so they competed to capture variability within the residual BOLD data. Signal components that correlated with K_{i-1} (Fig. 7A) were located cortically, broadly distributed throughout right hemispheric regions associated with the formation and maintenance of sensorimotor memories (Gazzaley et al., 2004; Lenartowicz and McIntosh, 2005): in dorsal prefrontal cortex (pre-PMd) and in anterior cingulate, middle temporal, and fusiform cortices, areas thought to interconnect with the basal ganglia and/or cerebellum (e.g. Bostan et al., 2010; Goldman-Rakic, 1988; Hoshi et al., 2005; Hoover and Strick, 1993, 1999; Kelly and Strick, 2003; Middleton and Strick, 1998; Middleton and Strick, 2001; Selemon and Goldman-Rakic, 1988). Moreover, memory-related activity in the septal area is consistent with engagement of a septo-hippocampal system important for maintenance of spatial memories (Olton, 1977). BOLD signal components correlating with K_{i-2} also spanned neocortex (Fig. 7B): right superior- (i.e. pre-SMA, BA 6) and inferior- (BA 44) frontal gyri, pre-PMd (BA 6), middle temporal (BA 21) and fusiform cortices; left prefrontal (BA 46), superior parietal, middle temporal (BA 37) and posterior cingulate cortices (BA 23). Areas with activities correlated with K_{i-2} did not overlap with those correlated with K_{i-1} . We also observed memory-model correlations with both K_{i-1} and K_{i-2} in the right parahippocampal cortex (BA 36); parahippocampal cortex is part of an interconnected network of prefrontal and hippocampal formation regions (Goldman-Rakic et al., 1984) thought to play a critical role in the encoding/retrieval (Burgess et al., 2002) and maintenance of novel, short-term sensorimotor memories (Hasselmo and Stern, 2006; Ranganath and D'Esposito, 2001; for a review see Eichenbaum, 2000), particularly those of spatial locations within a visual scene (but see also Eichenbaum et al., 1999).

In the *prediction model* (Fig. 8), K_{i-1} and K_{i-2} entered the regression in a subject-specific proportion corresponding to our best estimate of his or her prediction of the upcoming load (Eq. (4)) and so the two memory terms did not compete for data variance in the analysis. We found high-confidence correlation with \hat{K}_i in the left cerebellar hemisphere (lobules VI and VIII/IX), regions thought to contribute to internal representation of novel hand-held tool behaviors (Diedrichsen et al., 2005; Imamizu et al., 2000, 2003; Kawato et al., 2003; for a review see Wolpert et al., 1998), reward-based behavioral learning (Haruno et al., 2004) and, potentially, the prediction of neural events (Dugas and Smith, 1992; see also Coenen and Sejnowski, 1996; for a review see Courchesne and Allen, 1997). High confidence clusters were also located bilaterally in the region of the red nuclei, which receive cerebellar output through the deep cerebellar nuclei (Courville, 1966; cf. Glickstein et al., 2011; for review and discussion see Kennedy, 1990) and which influence spinal gamma motor neurons via the rubrospinal and rubrobulbospinal tracts (Appelberg, 1962a, 1962b; Appelberg et al., 1975; Johansson, 1988). The red nuclei also send projections back to the cerebellum via the principal olive (Appelberg, 1967; Jeneskog, 1974; Nathan and Smith, 1982), a pathway that appears to play an important role in the control of limb posture (Kennedy et al., 1982) and movement (Jeneskog, 1974). Several smaller clusters were observed in the right substantia nigra, globus pallidus and centromedian nucleus of the thalamus. These nuclei contribute to cortico-striatal and thalamo-striatal "loops" (Glimcher and Lau, 2005; Ilinsky et al., 1985; Matsumoto et al., 2001) thought to be involved in reward-optimizing behaviors (Middleton and Strick, 2001; Schultz et al., 1993; see also Schultz et al., 1995) and the selection of actions in response to unexpected stimuli (Matsumoto et al., 2001; Minamimoto et al., 2005, 2009; see also Tunik et al., 2009). Additional BOLD signal correlations with \hat{K}_i were found in the region of the hippocampus, an area thought to be important for the formation of spatial memories (Mahut, 1971), maps of the body in space (Nadel, 1991; Nadel and MacDonald, 1980) and "memory spaces" (Eichenbaum et al., 1999), as well as in the anterior and posterior intraparietal sulcus, areas involved in the estimation of dynamic limb state and prediction of the sensorimotor consequences of motor commands (Desmurget et al., 1999; Tunik et al., 2005), the on-line feedback control of goal-directed actions (Tunik et al., 2005) and the multimodal sensory integration (Beauchamp et al., 2010) required for a mixed body- and gaze-centered spatial encoding of motor goals (Bernier and Grafton, 2010).

Table 4
Single-subject analysis of predictive BOLD activity. Significance of linear term (slope).

Subject	GP	HIP	CER
1	***	***	***
2	*		
3	**		
4			
5			**
6			
7	*	***	***
8	**	**	**
9		***	
10	*	***	*
11	*	***	**
12		**	
14	**	***	***
15			
16	***		***
17		*	***
18	***	***	*
20	**		

*** $p \leq 0.05$; ** $p \leq 0.10$; * $p \leq 0.15$.

BOLD signal components correlating with \hat{K}_i overlapped with two regions identified in the memory model analysis [right pre-PMd and middle temporal gyrus (BA 21)] but were distinct in other cortical areas including the right hippocampus, right superior parietal lobule (anterior and posterior intraparietal sulcus, IPS; BA 7) and left fusiform gyrus (BA 37). In pre-PMd, a comparison of MSE values from the two models revealed a slight explanatory advantage for the memory model over the prediction model (memory model: median $MSE = 343\%^2$, range: 81 to $1235\%^2$; prediction model: median $MSE = 345\%^2$, range: 82 to $1242\%^2$; 1-sample sign test on the intrasubject difference between MSE values: $p < 0.0005$). However, when we account for the memory model's additional degree of freedom (Bohlin, 1978; cf. Ljung, 1999 p. 508), we find no compelling evidence to reject the prediction model as the most parsimonious explanation of the data variance. Based on this equivocal outcome, we cannot conclude whether activity in pre-PMd corresponds to the storage/recall of sensorimotor memories needed to compose a prediction of upcoming loads or the composition of that prediction itself. We also found equivocal results for the MTG overlap region.

In regions of interest throughout the brain, the relationship between the regressor magnitude and BOLD signal change was approximately linear (Fig. 9). The linearization of kinematic performance about the operating point defined by the currently predicted load (Fig. 4B) was matched by a corresponding linear relationship between BOLD signal change and the behavioral variables contributing to that prediction. For example, the BOLD signal varied by $3.5\% \pm 6.2\%$ across the range of K_i values in the cerebellar cortex (across-subjects mean \pm SD, $n = 18$), by $1.9\% \pm 4.9\%$ across the range of K_{i-1} values in MFG, by $1.4\% \pm 7.7\%$ with variation in K_{i-2} in FG, by $4.8\% \pm 8.7\%$ with variation in $|\epsilon_i|$ in the PUT and by $4.5\% \pm 6.7\%$ with variation in \hat{K} in the GP. We then evaluated the extent to which the population trends of Figs. 8 and 9 reflected predictive neural activity within individual subjects (Table 4). We performed within-subject fits of a linear equation to the binned (regressor α_i , response β_i) data within GP, HIP and CER. We considered as significant those fits with linear trends with $p \leq 0.1$. Out of 18 subject datasets analyzed, three demonstrated predictive activity in all three regions of interest (GP, HIP and CER), four subjects had predictive activity in two out of the three regions whereas seven subjects had predictive activity in just one of them. We found no compelling evidence of predictive BOLD signals in four subjects. Thus, subjects were just as likely to exhibit predictive activity in multiple neuroadaptive systems as they were to have it in just one. Subjects were unlikely to exhibit no predictive

activity in any of these regions. There was no clear grouping of subjects according to which regions displayed predictive signals: For subjects exhibiting multiple predictive responses at $p \leq 0.1$, four displayed the combination GP and HIP, four had the combination GP and CER, whereas five had the combination HIP and CER. Although the absolute counts differ somewhat if we instead use a significance threshold that is more strict ($p \leq 0.05$) or more liberal ($p \leq 0.15$), the relative frequency of single vs. multiple predictive responses would not change meaningfully.

Discussion

Subjects performed goal-directed wrist movements against spring-like loads that varied randomly from one trial to the next. Although the loads were in fact unpredictable, subjects tried to use sensorimotor memories from recent movements to predict and compensate for upcoming loads (Fig. 4C). These predictions enabled subjects to adapt performance so that the task was accomplished, on average, with a minimum of effort (Fig. 4A, inset). Using an approach proposed by Scheidt and colleagues (Scheidt et al., 2001), we estimated each subject's prediction of upcoming load based solely on performance variables observed during the most recent trials. We used these estimates to identify neural correlates of memory-based sensorimotor prediction – a subject-specific 'signature' of prediction within the neuromotor system (Eq. (4)). We used this time series, along with others reflecting trial-by-trial modulations in perturbation strength and performance errors, as inputs to a set of event-related analyses of the functional MR images obtained as subjects practiced the visual target capture task. The input time series were crafted (and verified) to be statistically independent, thereby enabling us to decompose, sequentially, the overall BOLD signal into components related only generally to performance of the task (Fig. 5), components correlating with current-trial variations in performance (Fig. 6), and components related to the storage/recall (Fig. 7) and integration (Fig. 8) of sensorimotor memories. The analyses revealed a distributed, bilateral network of cortical and subcortical activity supporting predictive compensation for changing environmental loads during visual target capture. Cortical regions exhibited trial-by-trial fluctuations in BOLD signal consistent with the associative storage and recall of task-relevant sensorimotor memories or "states" (Figs. 6A and 7); bilateral activations in associative regions of the striatum were consistent with reward-optimizing reinforcement learning (Fig. 6B); activity in the cerebellar cortex implicated this structure in both the online (Figs. 5 and 6A) and predictive (Fig. 8) compensation for environmental disturbances. These results suggest active engagement of each of the three primary neuroadaptive mechanisms thought to contribute to motor learning and adaptation (Doya, 1999, 2000; Houk and Wise, 1995). Importantly, BOLD signatures of memory-based prediction of upcoming load were not limited to the cerebellum, but were also observed in an output pathway of the basal ganglia and in several cortical areas, including the hippocampus and posterior parietal cortex. Analysis of individual subject images in these regions found that subjects were just as likely to exhibit predictive activity in multiple regions, as they were to display it in one. Although the multiplicity of predictive activity might have been due, in part, to the highly-constrained nature of our task (discussed in Strategies section below), the results demonstrate that compensation for environmental load relies on contributions from multiple neuroadaptive mechanisms.

BOLD signal correlates of current sensorimotor state

By design, the applied load K_i correlated strongly with peak torque applied to the subject's hand during wrist flexion. Because neuromuscular control of the wrist is compliant, K_i also correlated with "signed" kinematic error: subjects undershot the goal (a negative error) when the load was stiffer than average and overshot the goal (positive error) when the load was more compliant than average

(Fig. 4B). A limitation of the regression analyses we used is that they cannot determine whether BOLD signals that correlate with K_i actually depend on load, error, or some combination of factors that co-vary with load. The *Level-2* analysis identified K_i -related activities in areas previously implicated in the representation and online (moment-by-moment) compensation for kinematic performance errors, including left primary sensorimotor and right inferior parietal and anterior cingulate cortices as well as right cerebellar lobules V–VI (cf. Diedrichsen et al., 2005; Suminski et al., 2007a; see also Jueptner et al., 1997). The same analysis also identified activities in areas implicated in the production of graded force at the hand: primary sensorimotor, premotor, and anterior cingulate cortices (cf. Cramer et al., 2002; Dai et al., 2001; Vaillancourt et al., 2003; Ward et al., 2008). Although the question of whether cortical neurons encode information related to movement kinematics or kinetics has received great interest (Georgopoulos et al., 1989; Georgopoulos et al., 1992; Kalaska et al., 1989; Moran and Schwartz, 1999; but see also Hatsopoulos et al., 2007), recent theoretical and experimental evidence suggests that the brain adjusts its neural tunings (feedback sensitivities) according to prevailing task demands (i.e. optimal feedback control: cf. Loeb et al., 1990; Loeb and Marks, 1985; Scott, 2004; Todorov and Jordan, 2002). Consistent with this idea, a recent fMRI study found that separate brain regions contribute to the moment-by-moment feedback regulation of wrist angle during a stabilization task and the adjustment of feedback set-point and/or sensitivity on a longer time scale when the moment-by-moment control fails to achieve subjective performance criteria (Suminski et al., 2007a). The fact that the regressor K_i (commanded load) correlates with signed kinematic error (ε_i) is not a limitation in our analysis, but rather makes K_i an ideal proxy for whatever kinematic or kinetic sensorimotor states contribute to feedback control in our task.

Mechanisms supporting predictive compensation during visually-directed movement

Predictive compensations must be guided by past experience if they are to be effective in improving performance. Even trial-and-error exploration requires storage of recent performance information so that actions with greater reward are repeated. Behavioral analysis (Fig. 4) identified K_{i-1} and K_{i-2} as a minimal set of memories/states contributing to trial-by-trial evolution of performance observed in our task. Image analysis found K_{i-1} and K_{i-2} represented in multiple, widely-separated, and non-overlapping regions in the right hemisphere, including prefrontal (pre-PMd) and temporal (MTG) association areas, cingulate cortex, septum and parahippocampal areas. These results are consistent with the idea that a fundamental role of cortex is to encode states of behavioral significance (Doya, 1999, 2000; Houk and Wise, 1995). More specifically, they are consistent with studies exploring the neural basis of working memory (for reviews see Eichenbaum, 2000; Fuster, 2009; see also Ullman, 2004), which implicate reentrant cortical–cortical and cortico–subcortical loops in the storage and maintenance of memoranda. Unit recording evidence in animals and functional imaging and lesion studies in humans demonstrate that memory networks are “largely interregional, linking neuron assemblies and smaller networks in separate and noncontiguous areas of the cortex” (Fuster, 2009). Procedural memory, which facilitates the learning and adaptation of sensorimotor skills, is mediated by prefrontal and middle temporal cortices, in connection with anterior putamen and caudate (Knowlton et al., 1996; Miyachi et al., 2002). In contrast, prefrontal, parietal, septal, parahippocampal and thalamic areas contribute to the formation and maintenance of episodic memories (of personal experience) and spatial memories (of object location; for reviews see Aggleton and Brown, 1999; Burgess et al., 2002; Fuster, 2009) and to the consolidation of new declarative memories (memories that can be held in consciousness; cf. Tulving, 1987). Because these forms of memory may be important during the initial stages of adapting to a novel visuomotor perturbation

(cf. Anguera et al., 2009; Keisler and Shadmehr, 2010; see also Redding and Wallace, 2002), both may have contributed importantly to subject performance in our persistently novel task.

Although activation sites for K_{i-1} were adjacent to those for K_{i-2} in executive and sensory association cortices (pre-PMd and MTG), they were non-overlapping in other areas (cingulate, fusiform and inferior frontal cortices, septum). This result implies a distributed network encoding of serial order in goal-directed reaching. That is, as information cascades through working memory, it shifts from circuits associated with the most recent movement attempt to circuits representing events further in the past.

Predictive BOLD signals based on these memories were located in cerebral cortex [including right hippocampus, right posterior parietal (anterior IPS) and right PMd cortices], in the right globus pallidus and centromedian nucleus of the thalamus (an output pathway of the basal ganglia) and in the left cerebellar cortex (lobule VI) and bilaterally in the red nucleus. These regions are thought to play very different roles in the planning and control of sensory-guided movements. In addition to its role in declarative memory formation in general, the right hippocampal system is also believed important for forming spatial memories and/or “maps of the body in space” (Piekema et al., 2006; but see also Eichenbaum et al., 1999), information that is conveyed to neocortical association areas via cingulate cortex (Sutherland et al., 1988) for possible use in determining which joints to move, in which direction. In contrast, anterior intraparietal cortex plays a critical role in the estimation of dynamic limb state for use in the prediction of the sensorimotor consequences of motor commands (Desmurget et al., 1999; Tunik et al., 2005) and the on-line feedback control of goal-directed actions (Tunik et al., 2005; see also Suminski et al., 2007a). The basal ganglia play a critical role in selecting movements (Graybiel, 1998; Gurney et al., 2001a, 2001b; Houk, 2011; Tunik et al., 2009) and in the scaling of movement amplitudes (Desmurget et al., 2004; Krakauer et al., 2004; see Jueptner and Weiller, 1998). The cerebellum is implicated in the ongoing feedback regulation of limb position (Eccles, 1967; Mackay and Murphy, 1979), in the predictive cancellation of sensory afference (Blakemore et al., 1998, 2001; see also Serrien and Wiesendanger, 1999) and in the adaptation to novel visuomotor (Imamizu et al., 2000, 2003, 2004, 2007; Seidler et al., 2004; Tseng et al., 2007) and dynamic environments (Diedrichsen et al., 2005; Shadmehr and Holcomb, 1997) that require complex adjustments in the coordination of phasic activations in muscles driving limb motion (see Krakauer et al., 2004; see also Liu et al., 2011). How might these predictive signals have contributed to adaptive control in the present experiments?

Strategies...

At least three different adaptive strategies could have been used to solve the visual target capture task. First, subjects could have implemented a spatial remapping strategy to capture the target. Here, the appropriate response to overshoot (undershoot) would be to move the internal representation of the target closer to (farther from) the starting point of the hand. As the right hippocampus is thought to be involved in storing and maintaining the topographic memory (spatial map) needed to move to a remembered goal (Maguire et al., 1996, 1998; Nadel and MacDonald, 1980; Vargha-Khadem et al., 1997; for a review see Burgess et al., 2002), our data suggest that subjects may have recruited the hippocampus to remap the visuospatial relationship between visually-perceived target distance and desired movement extent. Cingulate cortex conveys hippocampal information to neocortical association areas (Sutherland et al., 1988), thus providing a means by which the hippocampus could influence the spatial planning of subsequent movements (cf. Andersen and Buneo, 2002). We also found two clusters of predictive activity in the right SPL around the IPS, one located near the parieto-occipital junction and the other located more anteriorly – areas previously shown to display reach-related activity (Bernier and Grafton, 2010; Filimon et al., 2009). Our observations are consistent

with the idea that posterior parietal cortex plays a critical role in multimodal sensory integration for spatially directed action (Avillac et al., 2005; Bisley and Goldberg, 2003, 2010; Prevosto et al., 2010). Spatial remapping could be part of a ‘fast’ compensatory response to kinematic error that shares critical resources with the declarative memory system (Keisler and Shadmehr, 2010).

Second, because the manipulandum constrained the wrist in all dimensions except the task-relevant degree-of-freedom, subjects could have compensated for target overshoot (undershoot) by decreasing (increasing) the amplitude of any preexisting pattern of feed-forward motor commands inducing wrist flexion. A large body of evidence suggests that the basal ganglia play a vital role in selecting which movement to make in a given circumstance and in planning/controlling the selected movement’s amplitude (Desmurget et al., 2003, 2004; Krakauer et al., 2004; see also Houk, 2011). In our experiments, anterior putamen, globus pallidus and substantia nigra all demonstrated strong activity related to reward, prediction error and/or other error correction processes that are dependent on the magnitude but not sign of kinematic errors. Moreover, the observation of predictive activity in right CM thalamus is suggestive because this structure receives projections from the globus pallidus and sends reciprocal projections back to striatum (Glimcher and Lau, 2005; Matsumoto et al., 2001; McLardy, 1948), thus providing a way for load predictions in the basal ganglia to influence movement selection and/or amplitude planning on the subsequent movement attempt (see Schultz et al., 1995; see also Minamimoto et al., 2005).

Third, subjects could have adapted to the novel spring-like dynamics of the manipulandum by adjusting coordination among the multiple muscles spanning the wrist. Numerous experimental, lesion, and theoretical/modeling studies implicate the cerebellum in the sensorimotor adaptation and learning of coordinated movement (for example: Bastian et al., 1996; Imamizu et al., 2000, 2003, 2004; Martin et al., 1996; Thach, 1996; see also Miller and Sinkjaer, 1998; Tseng et al., 2007). In one model of cerebellar function (Imamizu et al., 2003; Kawato and Gomi, 1992; Wolpert and Kawato, 1998), a feedback controller, in conjunction with an inverse model of the controlled object, transforms a desired trajectory of the arm into an appropriate set of motor commands. Learning an accurate inverse model is facilitated by action of the feedback controller, which transforms trajectory error into a feedback motor command that can both augment the ongoing movement and train the inverse model used to generate the commands in the first place. The controller also includes a forward model that takes as input the current state of the arm and an efferent copy of motor commands (von Holst and Mittelstaedt, 1950, as cited in von Holst, 1996) and produces an estimate of the new state of the arm. One possible use for the predictions provided by a forward model is to serve as an estimate of sensory signals during the delay associated with sensory transduction and transport (Bell et al., 2008; Ebner and Pasalar, 2008; Miall et al., 1993; Wolpert et al., 1995).

The observation of bilateral predictive activity in the mesodiencephalic area of the red nucleus in the current study suggests another use for predictive signals. Recall that the red nuclei are an important output channel of the cerebellum that receives projections from the deep cerebellar nuclei (Courville, 1966; cf. Glickstein et al., 2011) and send projections back to the cerebellar nuclei and cortex via the principal olive (Appelberg, 1967; DeZeeuw et al., 1998; Nathan and Smith, 1982; Onodera, 1984). The red nuclei also send descending projections to the spinal cord, where they act primarily on gamma motor neurons γ MNs (Appelberg et al., 1975; Johansson, 1988) to encode the dynamics of limb muscle activity (Miller and Sinkjaer, 1998). Whereas the reciprocal connections may provide a way for current load predictions to influence cerebellar feedback control of ongoing movement, the descending projections provide a means for the cerebellum to assert *conditional feedback control* over the movement (see Houk and Rymer, 1981). Accordingly, the cerebellum need not produce the primary motor commands that drive limb

motion via extrafusal muscle fiber activation (although it may play a primary role in the learning of these commands). Instead, we take the traditional view that the cerebellum serves as an “accessory adjuster” to primary motor commands generated elsewhere, for example primary motor cortex (MacKay and Murphy, 1979). Based on our observations, we speculate that predictive mechanisms in lateral cerebellar cortex compute motor commands sent to γ MNs, which innervate intrafusal muscle fibers that give rise to muscle spindle afferents. As noted by Houk and Rymer (1981), the intrinsic parallel configuration of intrafusal and extrafusal muscle fibers make muscle spindles ideal model reference error detectors – elements designed to “cancel” expected sensory feedback signals under conditions in which the controlled system (the extrafusal muscle fibers) responds precisely as does the model (the intrafusal fibers).

In conditional feedback control, movement control is exclusively feed-forward except when disturbances interfere with ideal performance, thus producing a model reference error signal (see Houk and Rymer, 1981). For this to work, however, γ -drive to the intrafusal fibers must predict the response of the limb as coupled to its (variable) external load – which can only occur if the γ command is itself adaptive. The cerebellar and red nucleus activity we observed (Fig. 8) could be the origins of this adaptive command. Since spindle feedback projects back to the cerebellum via the spinocuneocerebellar tract, it is possible that conditional error signals originating from muscle spindles could be used to drive online feedback corrections (the conditional feedback control of Houk and Rymer, 1981) and/or to update the forward and inverse models that may have been used to learn the commands in the first place (Fagg et al., 1997; Kawato and Gomi, 1992).

...Speculations...

All three of these compensatory strategies are viable solutions to our visual target capture task. To the extent that predictive BOLD activity in the hippocampal and posterior parietal cortices, basal ganglia and cerebellum reflect the different adaptive approaches, the pattern of activations displayed in Table 4 suggests that all three may have been recruited to compensate for the imposed loads. For example, movement planning in frontal parietal networks may have been conducted within a spatial reference frame established by the hippocampus and associated structures. The basal ganglia may then have selected one particular sequence and scaling of muscle activations (a feedforward motor program) likely to realize that plan. Finally, the cerebellum may have monitored the ongoing movement by predicting the sensory consequences of the evolving action and by initiating feedback corrections and internal model updates when the realized sensations deviated from expectation. Future studies should examine how the brain might integrate multiple predictive compensations to achieve a final overall motor response and whether the multiple predictive mechanisms identified here compete or cooperate to compensate for imposed environmental loads.

We observed two regions of overlap in the two *Level-3* analyses (right pre-PMd and right middle temporal gyrus). When we accounted for differences in model degrees of freedom, we found no compelling evidence to accept one model over the other in these areas and so, this activity equivocally corresponds to the representation of sensorimotor memories needed to compose a prediction of upcoming loads and/or the composition of that prediction itself. A previous PET study of motor adaptation and consolidation (Shadmehr and Holcomb, 1997) found activity “specific to the recall of a recently acquired internal model of the field” at nearly the same pre-PMd location as observed in our level-3 analyses, except in the *left*, not right, hemisphere (their Fig. 3B). In the experiments of Shadmehr and Holcomb, subjects were required to adapt to the novel dynamics of a viscous curl force field while moving a planar, 2-joint manipulandum in 8 different directions and so, they could not have adapted using either a simple rescaling of existing coordination patterns or a spatial remapping of the target relative to the hand’s starting location. In

contrast, a PET study by Krakauer and colleagues (Krakauer et al., 2004) and an fMRI study by Imamizu and colleagues (Imamizu et al., 2007) both found right-hemispheric premotor activity associated with visuomotor adaptation of right-handed movements in the presence of cursor rotation. Given the hemispheric difference between dynamic and visuomotor adaptations revealed by these previous studies and others (Sainburg, 2002; Sainburg and Kalakanis, 2000), the fronto-parietal activity observed in our *Level-3* analysis may well indicate that subjects in our study adopted a visuospatial solution to the movement task rather than a dynamic adaptation. Indeed, subjects may have been predisposed to this kind of solution because they were already forced to solve a novel visuospatial transformation: they were required to lay recumbent in a scanner while making flexion/extension movements of the wrist, movements that were translated into vertical motions of a visual cursor.

... and implications

This study provided direct experimental evidence that prediction of hand-held load is a distributed computation supported by a bilateral network of cortical and subcortical activity, thus reflecting active engagement of three neuroadaptive mechanisms previously implicated in motor learning and adaptation (cf. Doya, 1999, 2000; Houk and Wise, 1995): cortical regions for the storage and recall of task-relevant sensorimotor and visuospatial memories, basal-ganglionic networks for selecting and scaling movements to optimize reward or a related signal, and cerebellar pathways for both the online and predictive compensation for environmental disturbances. Based on neurophysiological considerations and evidence from the literature, we concluded that these predictions likely represent distinct computations within cerebellar, basal ganglionic and hippocampal loops that engage cortical working memory. Although multiplicity of representations of predictive activity may have been facilitated by the highly constrained nature of our task, the results nevertheless demonstrate that compensations for environmental load can recruit multiple neuroadaptive mechanisms. By disambiguating load prediction from the processing, storage/recall, and weighted integration of recent sensorimotor memories, the present study demonstrates a new experimental approach that can be exploited to advance understanding of how the neural systems supporting motor adaptation are altered by experience, neurologic disease and pharmacological intervention.

Acknowledgments

This work was supported by grants from the National Science Foundation BES0238442 and the National Institutes of Health NICHHD R01HD053727, NINDS R01NS053581 and NCRR GCRC M01RR00058. We are deeply grateful to Steve Rao of the Cleveland Clinic, who contributed extensive discussion and insight to a prior version of this manuscript. We would also like to thank Doug Ward and Sally Durgerian from the Medical College of Wisconsin for assistance in the statistical analysis of fMRI data.

Appendix A. Supplementary material

Supplementary data to this article can be found online at doi:10.1016/j.neuroimage.2011.07.072.

References

- Aggleton, J.P., Brown, M.W., 1999. Episodic memory, amnesia, and the hippocampal-anterior thalamic axis. *Behav. Brain Sci.* 22, 425–489.
- Alexander, G.E., DeLong, M.R., Strick, P.L., 1986. Parallel organization of functionally segregated circuits linking basal ganglia and cortex. *Ann. Rev. Neurosci.* 9, 357–381.
- Andersen, R.A., Buneo, C.A., 2002. Intentional maps in posterior parietal cortex. *Ann. Rev. Neurosci.* 25, 189–220.
- Angel, R.W., 1976. Efference copy in the control of movement. *Neurology* 26 (12), 1164–1168.
- Anguera, J.A., Reuter-Lorenz, P.A., Willingham, D.T., Seidler, R.D., 2009. Contributions of spatial working memory to visuomotor learning. *J. Cogn. Neurosci.* 22 (9), 1917–1930.
- Appelberg, B., 1962a. The effect of electrical stimulation of nucleus ruber on the gamma motor system. *Acta Physiol. Scand.* 55, 150–159.
- Appelberg, B., 1962b. The effect of electrical stimulation in nucleus ruber on the response to stretch in primary and secondary muscle spindle afferents. *Acta Physiol. Scand.* 56, 140–151.
- Appelberg, B., 1967. A rubro-olivary pathway. II. Simultaneous action on dynamic fusimotor neurones and the activity of the posterior lobe of the cerebellar cortex. *Exp. Brain Res.* 3 (1967), 382–390.
- Appelberg, B., Jenkinson, T., Johansson, H., 1975. Rubrospinal control of static and dynamic fusimotor neurones. *Acta Physiol. Scand.* 95, 431–440.
- Avillac, M., Deneve, S., Olivier, E., Pouget, A., Duhamel, J.-R., 2005. Reference frames for representing visual and tactile locations in parietal cortex. *Nat. Neurosci.* 8, 941–949.
- Bastian, A.J., Martin, T.A., Keating, J.G., Thach, W.T., 1996. Cerebellar ataxia: abnormal control of interaction torques across multiple joints. *J. Neurophysiol.* 76 (1), 492–509.
- Beauchamp, M.S., Pasalar, S., Ro, T., 2010. Neural substrates of reliability-weighted visual-tactile multisensory integration. *Front. Syst. Neurosci.* 4 (25), 1–11.
- Bell, C.C., Han, V., Sawtell, N.B., 2008. Cerebellum-like structures and their implications for cerebellar function. *Ann. Rev. Neurosci.* 31, 1–24.
- Bernier, P.-M., Grafton, S.T., 2010. Human posterior parietal cortex flexibly determines reference frames for reaching based on sensory context. *Neuron* 68, 776–788.
- Bigland-Ritchie, B., Woods, J.J., 1984. Changes in muscle contractile properties and neural control during human muscular fatigue. *Muscle Nerve* 7, 691–699.
- Bisley, J.W., Goldberg, M.E., 2003. Neuronal activity in the lateral intraparietal area and spatial attention. *Science* 299, 81–86.
- Bisley, J.W., Goldberg, M.E., 2010. Attention, intention, and priority in the parietal lobe. *Ann. Rev. Neurosci.* 33, 1–21.
- Blakemore, S.J., Wolpert, D.M., Frith, C.D., 1998. Central cancellation of self-produced tickle sensation. *Nat. Neurosci.* 1 (7), 635–640.
- Blakemore, S.J., Frith, C.D., Wolpert, D.M., 2001. The cerebellum is involved in predicting the sensory consequences of action. *NeuroReport* 12, 1879–1884.
- Bland, B.H., Oddie, S.D., 2001. Theta band oscillation and synchrony in the hippocampal formation and associated structures: the case for its role in sensorimotor integration. *Behav. Brain Res.* 127, 119–136.
- Bohlin, T., 1978. Maximum-power validation of models without higher-order fitting. *Automatica* 14, 137–146.
- Bostan, A., Dum, R., Strick, P., 2010. The basal ganglia communicates with the cerebellum. *PNAS* 107 (18), 8452–8456.
- Boussaoud, D., 2001. Attention versus intention in the primate premotor cortex. *NeuroImage* 14, S40–S45.
- Boyd, L.A., Winstein, C.J., 2004. Cerebellar stroke impairs temporal but not spatial accuracy during implicit motor learning. *Neurorehabil. Neural Repair* 18, 134–143.
- Buneo, C.A., Andersen, R.A., 2006. The posterior parietal cortex: sensorimotor interface for the planning and online control of visually guided movements. *Neuropsychology* 44, 2594–2606.
- Burgess, N., Maguire, E.A., O'Keefe, J., 2002. The human hippocampus and spatial and episodic memory. *Neuron* 35, 625–641.
- Bursztyn, L.L.C.D., Ganesh, G., Imamizu, H., Kawato, M., Flanagan, J.R., 2006. Neural correlates of internal-model loading. *Curr. Biol.* 16, 2440–2445.
- Carroll, L., 1871. *Through the Looking-Glass, and What Alice Found There*. Random House, New York, p. 73.
- Coenen, O.J.M.D., Sejnowski, T.J., 1996. Learning to make predictions in the cerebellum may explain the anticipatory modulation of the vestibulo-ocular reflex (VOR) gain with vergence. *Proc 3rd Joint Symp Neural Comp.* Pasadena CA, pp. 1–20.
- Cohen, M.S., 1997. Parametric analysis of fMRI data using linear systems methods. *NeuroImage* 6, 93–103.
- Cohen, N.J., Eichenbaum, H., 1991. The theory that wouldn't die: a critical look at the spatial mapping theory of hippocampal function. *Hippocampus* 1 (3), 265–268.
- Courchesne, E., Allen, G., 1997. Prediction and preparation, fundamental functions of the cerebellum. *Learn. Mem.* 4, 1–35.
- Courville, J., 1966. Somatotopical organization of the projection from the nucleus interpositus anterior of the cerebellum to the red nucleus. An experimental study in the cat with silver impregnation methods. *Exp. Brain Res.* 2, 191–215.
- Cox, R.W., 1996. AFNI software for analysis and visualization of functional magnetic resonance neuroimages. *Comput. Biomed. Res.* 29, 162–173.
- Cramer, S.C., Weisskoff RM, J.D., Nelles, G., Foley, M., Finklestein, S.P., Rosen, B.R., 2002. Motor cortex activation is related to force of squeezing. *Hum. Brain Mapp.* 16, 197–205.
- Dai, T.H., Liu, J.Z., Sahgal, V., Brown, R.W., Yue, G.H., 2001. Relationship between muscle output and functional MRI-measures brain activation. *Exp. Brain Res.* 140, 290–300.
- Desmurget, M., Epstein, C.M., Turner, R.S., Prablanc, C., Alexander, G.E., Grafton, S.T., 1999. Role of the posterior parietal cortex in updating reaching movements to a visual target. *Nat. Neurosci.* 2, 563–567.
- Desmurget, M., Grea, H., Grethe, J.S., Prablanc, C., Alexander, G.E., Grafton, S.T., 2001. Functional anatomy of nonvisual feedback loops during reaching: a positron emission tomography study. *J. Neurosci.* 21, 2919–2928.
- Desmurget, M., Grafton, S.T., Vindras, P., Grea, H., Turner, R.S., 2003. Basal ganglia network mediates the control of movement amplitude. *Exp. Brain Res.* 153, 197–209.
- Desmurget, M., Grafton, S.T., Vindras, P., Grea, H., Turner, R.S., 2004. The basal ganglia network mediates the planning of movement amplitude. *Eur. J. Neurosci.* 19, 2871–2880.
- D'Esposito, M.D., Detre, J.A., Alsop, D.C., Shin, R.K., Atlas, S., Grossman, M., 1995. The neural basis of the central executive system of working memory. *Nature* 378, 279–281.

- DeZeeuw, C.I., Simpson, J.I., Hoogenraad, C.C., Galjart, N., Koekkoek, S.K.E., Ruigrok, T.J.H., 1998. Microcircuitry and function of the inferior olive. *Trends Neurosci.* 21, 391–400.
- Dieber, M.-P., Ibanez, V., Honda, M., Sadato, N., Raman, R., Hallett, M., 1998. Cerebral processes related to visuomotor imagery and generation of simple finger movement studies with positron emission tomography. *NeuroImage* 7, 73–85.
- Diedrichsen, J., Hashambhoy, Y., Rane, T., Shadmehr, R., 2005. Neural correlates of reach errors. *J. Neurosci.* 25, 9919–9931.
- Doya, K., 1999. What are the computations of the cerebellum, the basal ganglia and the cerebral cortex? *Neural Netw.* 12, 961–974.
- Doya, K., 2000. Complementary roles of basal ganglia and cerebellum in learning and motor control. *Curr. Opin. Neurobiol.* 10, 732–739.
- Doyon, J., Penhune, V., Ungerleider, L.G., 2003. Distinct contribution of the cortico-striatal and cortico-cerebellar systems to motor skill learning. *Neuropsychology* 41, 252–262.
- Doyon, J., Bellec, P., Amsel, R., Penhune, V., Monchi, O., Carrier, J., Lehericy, S., Benali, H., 2009. Contributions of the basal ganglia and functionally related brain structures to motor learning. *Behav. Brain Res.* 199, 61–75.
- Draper, N.R., Smith, H., 1998. *Applied Regression Analysis*, 3rd Ed. Wiley, New York, pp. 429–430.
- Dugas, C., Smith, A.M., 1992. Responses of cerebellar Purkinje cells to slip of a hand-held object. *J. Neurophysiol.* 67 (3), 483–495.
- Dypvik, A.T., Bland, B.H., 2004. Functional connectivity between the red nucleus and the hippocampus supports the role of hippocampal formation in sensorimotor integration. *J. Neurophysiol.* 92, 2040–2050.
- Ebner, T.J., Pasalar, S., 2008. Cerebellum predicts the future motor state. *Cerebellum* 7, 583–588.
- Eccles, J.C., 1967. Circuits in the cerebellar control of movement. *PNAS* 58 (1), 336–343.
- Eichenbaum, H., 2000. A cortical-hippocampal system for declarative memory. *Nat. Rev. Neurosci.* 1, 41–50.
- Eichenbaum, H., Dudchenko, P., Wood, E., Shapiro, M., Tanila, H., 1999. The hippocampus, memory, and place cells: is it spatial memory or a memory space? *Neuron* 23, 209–226.
- Emken, J.L., Reinkensmeyer, D.J., 2005. Robot-enhanced motor learning: accelerating internal model formation during locomotion by transient dynamic amplification. *IEEE Trans. Neural Syst. Rehabil. Eng.* 13 (1), 33–39.
- Evarts, E.V., Fromm, C., 1981. Transcortical reflexes and servo control of movement. *Can. J. Physiol. Pharmacol.* 59, 757–775.
- Evarts, E.V., Tanji, J., 1976. Reflex and intended responses in motor cortex pyramidal tract neurons of monkey. *J. Neurophysiol.* 39, 1069–1080.
- Fagg, A.H., Sitkoff, N., Barto, A.G., Houk, J.C., 1997. Cerebellar learning for control of a two-link arm in muscle space. *Proc. IEEE Intern Conf Robot Automat. Albuquerque, NM*, pp. 2638–2644.
- Filimon, F., Nelson, J.D., Huang, R.-S., Sereno, M.I., 2009. Multiple parietal reach regions in humans: cortical representation for visual and proprioceptive feedback during on-line reaching. *J. Neurosci.* 29, 2961–2971.
- Flanagan, J.R., Rao, A.K., 1995. Trajectory adaptation to a nonlinear visuomotor transformation: evidence of motion planning in visually perceived space. *J. Neurophysiol.* 74, 2174–2178.
- Fuster, J.M., 2009. Cortex and memory: emergence of a new paradigm. *J. Cogn. Neurosci.* 21 (11), 2047–2072.
- Fuster, J.M., Alexander, G.E., 1971. Neuron activity related to short-term memory. *Science* 173, 652–654.
- Gandolfo, F., Li, C.-S.R., Padoa-Schioppa, C., Bizzi, E., 2000. Cortical correlates of learning in monkeys adapting to a new dynamical environment. *PNAS* 97 (5), 2259–2263.
- Gazzaley, A., Rissman, J., D'Esposito, M., 2004. Functional connectivity during working memory maintenance. *Cogn. Affect. Behav. Neurosci.* 4 (4), 580–599.
- Georgopoulos, A.P., Lurito, J.T., Petrides, M., Schwartz, A.B., Massey, J.T., 1989. Mental rotation of the neuronal population vector. *Science* 243, 234–236.
- Georgopoulos, A.P., Ashe, J., Smyrnis, N., Taira, M., 1992. The motor cortex and the coding of force. *Science* 256, 1692–1695.
- Gilbert, P.F.C., Thach, W.T., 1977. *Brain Res.* 128, 309–328.
- Glickstein, M., Sultan, F., Voogd, J., 2011. Functional localization in the cerebellum. *Cortex* 47, 59–80.
- Glimcher, P.W., Lau, B., 2005. Rethinking the thalamus. *Nat. Neurosci.* 8 (8), 983–984.
- Goldman-Rakic, P.S., 1988. Topography of cognition: parallel distributed networks in primate association cortex. *Ann. Rev. Neurosci.* 11, 137–156.
- Goldman-Rakic, P.S., Selemon, L.D., Schwartz, M.L., 1984. Dual pathways connecting the dorsolateral prefrontal cortex with the hippocampal formation and parahippocampal cortex in the rhesus monkey. *Neuroscience* 12 (3), 719–743.
- Grafton, S.T., Schmitt, P., Van Harn, J., Biedrichsen, J., 2008. Neural substrates of visuomotor learning based on improved feedback control and prediction. *NeuroImage* 39, 1383–1395.
- Graybiel, A.M., 1995. Building action repertoires: memory and learning functions of the basal ganglia. *Curr. Opin. Neurobiol.* 5, 733–741.
- Graybiel, A.M., 1998. The basal ganglia and chunking of action repertoires. *Neurobiol. Learn. Mem.* 70, 119–136.
- Graybiel, A.M., 2005. The basal ganglia: learning new tricks and loving it. *Curr. Opin. Neurobiol.* 15, 638–644.
- Graybiel, A.M., Kimura, M., 1995. Adaptive neural networks in the basal ganglia. In: Houk, James C., Davis, Joel L., Beiser, David G. (Eds.), *Models of Information Processing in the Basal Ganglia*. MIT Press, Cambridge, Massachusetts.
- Gribble, P.L., Scott, S.H., 2002. Overlap of internal models in motor cortex for mechanical loads during reaching. *Nature* 417, 938–941.
- Grinband, J., Hirsch, J., Ferrera, V.P., 2006. A neural representation of categorization uncertainty in the human brain. *Neuron* 49, 757–763.
- Grosse-Wentrup, M., Contreras-Vidal, J.L., 2007. The role of the striatum in adaptation learning: a computational model. *Biol. Cybern.* 96, 377–388.
- Gurney, K., Prescott, T.J., Redgrave, P., 2001a. A computational model of action selection in the basal ganglia. I. A new functional anatomy. *Biol. Cybern.* 84, 401–410.
- Gurney, K., Prescott, T.J., Redgrave, P., 2001b. A computational model of action selection in the basal ganglia. II. Analysis and simulation of behavior. *Biol. Cybern.* 84, 411–423.
- Haruno, M., Kawato, M., 2006. Heterarchical reinforcement-learning model for integration of multiple cortico-striatal loops: fMRI examination in stimulus-reward association learning. *Neural Netw.* 19, 1242–1254.
- Haruno, M., Kuroda, T., Doya, K., Toyama, K., Kimura, M., Samejima, K., Imamizu, H., Kawato, M., 2004. A neural correlate of reward-based behavioral learning in caudate nucleus: a functional magnetic resonance imaging study of a stochastic decision task. *J. Neurosci.* 24 (7), 1660–1665.
- Hasan, Z., 1986. Optimized movement trajectories and joint stiffness in unperturbed, inertially loaded movements. *Biol. Cybern.* 53, 373–382.
- Hasselmo, M.E., Stern, C.E., 2006. Mechanisms underlying working memory for novel information. *Trends Cogn. Sci.* 10 (11), 487–493.
- Hatsopoulos, N.G., Xu, Q., Amit, Y., 2007. Encoding of movement fragments in the motor cortex. *J. Neurosci.* 27 (19), 5105–5114.
- Hikosaka, O., Nakahara, H., Rand, M., Sakai, K., Lu, X., Nakamura, K., Miyachi, S., Doya, K., 1999. *Trends Neurosci.* 22, 464–471.
- Hikosaka, O., Takikawa, Y., Kawagoe, R., 2000. Role of the Basal ganglia in the control of purposive saccadic eye movements. *Physiol. Rev.* 80, 953–978.
- Hikosaka, O., Nakamura, K., Sakai, K., Nakahara, H., 2002. Central mechanisms of motor skill learning. *Curr. Opin. Neurobiol.* 12, 217–222.
- Hikosaka, O., Bromberg-Martin, E., Hong, S., Matsumoto, M., 2008. New insights on the subcortical representation of reward. *Curr. Opin. Neurobiol.* 18, 203–208.
- Hoover, J.E., Strick, P.L., 1993. Multiple output channels in the basal ganglia. *Science* 259, 819–821.
- Hoover, J.E., Strick, P.L., 1999. The organization of cerebellar and basal ganglia outputs to primary motor cortex as revealed by retrograde transneuronal transport of herpes simplex virus type 1. *J. Neurosci.* 19 (4), 1446–1463.
- Hoshi, E., Tremblay, L., Féger, J., Carras, P.L., Strick, P.L., 2005. The cerebellum communicates with the basal ganglia. *Nat. Neurosci.* 8 (11), 1491–1493.
- Houk, J.C., 2011. Chapter 8: action selection and refinement in subcortical loops through basal ganglia and cerebellum. In: Seth, A.K., Bryson, J., Prescott, T.J. (Eds.), *Modeling Natural Action Selection*. Cambridge University Press.
- Houk, J.C., Rymer, W.Z., 1981. Neural control of muscle length and tension. In: Brooks, V.B. (Ed.), *Handbook of Physiology*. American Physiological Society, Baltimore, pp. 257–323.
- Houk, J.C., Wise, S.P., 1995. Distributed modular architectures linking basal ganglia, cerebellum, and cerebral cortex: their role in planning and controlling action. *Cereb. Cortex* 2, 95–110.
- Houk, J.C., Basriani, C., Fansler, D., Fishbach, A., Fraser, D., Reber, P.J., Roy, S.A., Simo, L.S., 2007. Action selection and refinement in subcortical loops through basal ganglia and cerebellum. *Philos. Trans. R. Soc. B.* 362, 1573–1583.
- Ilinsky, I.A., Jouandet, M.L., Goldman-Rakic, P.S., 1985. Organization of the nigrothalamic system in the rhesus monkey. *J. Comp. Neurol.* 236, 315–330.
- Imamizu, H., Miyauchi, S., Tamada, T., Sasaki, Y., Takino, R., Putz, B., Yoshioka, T., Kawato, M., 2000. Human cerebellar activity reflecting an acquired internal model of a new tool. *Nature* 403, 192–195.
- Imamizu, H., Kuroda, T., Miyauchi, S., Yoshioka, T., Kawato, M., 2003. Modular organization of internal models of tools in the human cerebellum. *PNAS* 100 (9), 5461–5466.
- Imamizu, H., Kuroda, T., Yoshioka, T., Kawato, M., 2004. Functional magnetic resonance imaging examination of two modular architectures for switching multiple internal models. *J. Neurosci.* 24 (5), 1173–1181.
- Imamizu, H., Higuchi, S., Toda, A., Kawato, M., 2007. Reorganization of brain activity for multiple internal models after short but intensive training. *Cortex* 43, 338–349.
- Ito, M., 2000. Mechanisms of motor learning in the cerebellum. *Brain Res.* 886, 237–245.
- Ito, M., 2005. Bases and implications of learning in the cerebellum – adaptive control and internal model mechanism. *Prog. Brain Res.* 148, 95–109.
- Jeneskog, T., 1974. Parallel activation of dynamic fusiform neurons and a climbing fiber system from the cat brain stem. I. Effects from the rubral region. *Acta Physiol. Scand.* 91, 223–242.
- Johansson, H., 1988. Rubrospinal and rubrobulbosplinal influences on dynamic and static gamma-motoneurons. *Behav. Brain Res.* 28, 97–107.
- Jonides, J., Smith, E.E., Koeppe, R.A., Awh, E., Minoshima, S., Mintun, M.A., 1993. Spatial working memory in humans as revealed by PET. *Nature* 363, 623–625.
- Jueptner, M., Weiller, C., 1998. A review of differences between basal ganglia and cerebellar control of movements as revealed by functional imaging studies. *Brain* 121, 1437–1449.
- Jueptner, M., Frith, C.D., Brooks, D.J., Frackowiak, R.S.J., Passingham, R.E., 1997. Anatomy of motor learning. II. Subcortical structures and learning by trial and error. *J. Neurophysiol.* 77, 1325–1337.
- Kalaska, J.F., Cohen, D.A., Hyde, M.L., Prud'homme, M., 1989. A comparison of movement direction-related versus load direction-related activity in primate motor cortex, using a two-dimensional reaching task. *J. Neurosci.* 9, 2080–2102.
- Kawashima, R., Roland, P.E., O'Sullivan, B.T., 1995. Functional anatomy of reaching and visuomotor learning: a positron emission tomography study. *Cereb. Cortex* 5 (2), 111–122.
- Kawato, M., Gomi, H., 1992. A computational model of four regions of the cerebellum based on feedback-error learning. *Biol. Cybern.* 68, 95–103.
- Kawato, M., Furukawa, K., Suzuki, R., 1987. A hierarchical neural-network model for control and learning of voluntary movement. *Biol. Cybern.* 57, 169–185.
- Kawato, M., Kuroda, T., Imamizu, H., Nakano, E., Miyauchi, S., Yoshioka, T., 2003. Internal forward models in the cerebellum: fMRI study on grip force and load force

- coupling. In: Prablanc, C., Pelisson, D., Rossetti, Y. (Eds.), *Progress in Brain Research*, Vol. 142, pp. 171–188.
- Kayser, A.S., Buchsbaum, B.R., Erickson, D.T., D'Esposito, M., 2010. The functional anatomy of a perceptual decision in the human brain. *J. Neurophysiol.* 103, 1179–1194.
- Keisler, A., Shadmehr, R., 2010. A shared resource between declarative memory and motor memory. *J. Neurosci.* 30 (44), 14817–14823.
- Kelly, R.M., Strick, P.L., 2003. Cerebellar loops with motor cortex and prefrontal cortex of a nonhuman primate. *J. Neurosci.* 23 (23), 8432–8444.
- Kennedy, P.R., 1990. Corticospinal, rubrospinal and rubro-olivary projections: a unifying hypothesis. *Trends Neurosci.* 12, 474–479.
- Kennedy, P.R., Ross, H.-G., Brooks, V.B., 1982. Participation of the principal olivary nucleus in neocerebellar motor control. *Exp. Brain Res.* 47, 95–104.
- Knowlton, B.J., Mangels, J.A., Squire, L.R., 1996. A neostriatal habit learning system in humans. *Science* 273, 1399–1402.
- Krakauer, J.W., Ghilardi, M.-F., Mentis, M., Barnes, A., Veysman, M., Eidelberg, D., Ghez, C., 2004. Differential cortical and subcortical activations in learning rotations and gains for reaching: a PET study. *J. Neurophysiol.* 91, 924–933.
- Lackner, J.R., Dizio, P., 1994. Rapid adaptation to Coriolis force perturbations of arm trajectory. *J. Neurophysiol.* 72, 299–313.
- Lee, J.-Y., Schweighofer, N., 2009. Dual adaptation supports a parallel architecture of motor memory. *J. Neurosci.* 29 (33), 10396–10404.
- Lenartowicz, A., McIntosh, A.R., 2005. The role of anterior cingulate cortex in working memory is shaped by functional connectivity. *J. Cogn. Neurosci.* 17, 1026–1042.
- Li, C.-S.R., Padoa-Schioppa, C., Bizzi, E., 2001. Neuronal correlates of motor performance and motor learning in the primary motor cortex of monkeys adapting to an external force field. *Neuron* 30, 593–607.
- Linsker, R., 1988. Self-organization in a perceptual network. *Computer* 21, 105–117.
- Liu, X., Mosier, K.M., Mussa-Ivaldi, F.A., Casadio, M., Scheidt, R.A., 2011. Reorganization of finger coordination patterns during adaptation to rotation and scaling of a newly-learned sensorimotor transformation. *J. Neurophysiol.* 105, 454–473.
- Ljung, L., 1999. *System Identification—Theory for the User*, 2nd ed. Prentice Hall, Upper Saddle River, NJ.
- Loeb, G.E., Marks, W.B., 1985. Optimal control principles for sensory transducers. In: Boyd, I.A., Gladden, M.H. (Eds.), *The Muscle Spindle*. MacMillan, London, pp. 409–415.
- Loeb, G.E., Levine, W.S., He, J., 1990. Understanding sensorimotor feedback through optimal control. *Cold Spring Harbor Symposia on Quantitative Biol.* pp. 791–803 (Vol LV).
- Luecke, J., von der Malsburg, C., 2004. Rapid processing and unsupervised learning in a model of the cortical macrocolumn. *Neural Comput.* 16 (3), 501–533.
- MacKay, W.A., Murphy, J.T., 1979. Cerebellar modulation of reflex gain. *Prog. Neurobiol.* 13, 361–417.
- Maguire, E.A., Burke, T., Phillips, J., Staunton, H., 1996. Topographical disorientation following unilateral temporal lobe lesions in humans. *Neuropsychologia* 34, 993–1001.
- Maguire, E.A., Frith, C.D., Burgess, N., Donnett, J.G., O'Keefe, J., 1998. Knowing where things are: parahippocampal involvement in encoding object locations in virtual large-scale space. *J. Cogn. Neurosci.* 10 (1), 61–76.
- Mahut, H., 1971. Spatial and object reversal learning in monkeys with partial temporal lobe ablation. *Neuropsychologia* 9, 409–429.
- Martin, T.A., Keating, J.G., Goodkin, H.P., Bastian, A.J., Thach, W.T., 1996. Throwing while looking through prisms I. Focal olivocerebellar lesions impair adaptation. *Brain* 119, 1183–1198.
- Matsumoto, N., Minamimoto, T., Graybiel, A.M., Kimura, M., 2001. Neurons in the thalamic CM-PF complex supply striatal neurons with information about behaviorally significant sensory events. *J. Neurophysiol.* 85, 960–976.
- McLardy, T., 1948. Projection of the centromedian nucleus of the human thalamus. *Brain* 71 (3), 290–303.
- Miall, R.C., Weir, D.J., Wolpert, D.M., Stein, J.F., 1993. Is the cerebellum a Smith predictor? *J. Mot. Behav.* 25 (3), 203–216.
- Miall, R.C., Reckess, G.Z., Imamizu, H., 2001. The cerebellum coordinates eye and hand tracking movements. *Nat. Neurosci.* 4 (6), 638–644.
- Middleton, F.A., Strick, P.L., 1998. Cerebellar output: motor and cognitive channels. *Trends Cogn. Sci.* 2 (9), 348–354.
- Middleton, F.A., Strick, P.L., 2001. A revised neuroanatomy of frontal-subcortical circuits. In: Lichter, David G., Cummings, Jeffrey L. (Eds.), *Frontal-Subcortical Circuits in Psychiatric and Neurological Disorders*. Guilford Publications Ltd., New York, NY, pp. 44–58.
- Miller, L.E., Sinkjaer, T., 1998. Primate red nucleus discharge encodes the dynamics of limb muscle activity. *J. Neurophysiol.* 80, 59–70.
- Minamimoto, T., Hori, Y., Kimura, M., 2005. Complementary process to response bias in the centromedian nucleus of the thalamus. *Science* 308, 1798–1801.
- Minamimoto, T., Hori, Y., Kimura, M., 2009. Roles of the thalamic CM-PF complex — basal ganglia circuit in externally driven rebias of action. *Brain Res. Bull.* 78, 75–79.
- Mink, J.W., 1996. The basal ganglia: focused selection and inhibition of competing motor programs. *Prog. Neurobiol.* 50 (4), 381–425.
- Miyachi, S., Hikosaka, O., Lu, X., 2002. Differential activation of monkey striatal neurons in the early and late stages of procedural learning. *Exp. Brain Res.* 146, 122–126.
- Moran, D.W., Schwartz, A.B., 1999. Motor cortical representation of speed and direction during reaching. *J. Neurophysiol.* 82, 2676–2692.
- Nadel, L., 1991. The hippocampus and space revisited. *Hippocampus* 1 (3), 221–229.
- Nadel, L., MacDonald, L., 1980. Hippocampus: cognitive map or working memory? *Behav. Neural Biol.* 29, 405–409.
- Nathan, P.W., Smith, M.C., 1982. The rubrospinal and central tegmental tracts in man. *Brain* 105, 223–269.
- Nelson, W.L., 1983. Physical principles for economies of skilled movements. *Biol. Cybern.* 46, 135–147.
- O'Doherty, J.P., Dayan, P., Friston, K., Critchley, H., Dolan, R.J., 2003. Temporal difference models and reward-related learning in the human brain. *Neuron* 28, 329–337.
- Oldfield, R.C., 1971. The assessment and analysis of handedness: the Edinburgh inventory. *Neuropsychologia* 9, 97–113.
- Olton, D.S., 1977. The function of septo-hippocampal connections in spatially organized behavior. *CIBA Found. Symp.* 58, 327–349.
- Onodera, S., 1984. Olivary projections from the mesodiencephalic structures in the cat studied by means of axonal transport of horseradish peroxidase and titrated amino acids. *J. Comp. Neurol.* 227 (1), 37–49.
- Paus, T., 2001. Primate anterior cingulate cortex: where motor control, drive and cognition interface. *Nat. Rev. Neurosci.* 2, 417–424.
- Picard, N., Strick, P., 1996. Motor areas of the medial wall: a review of their location and functional activation. *Cereb. Cortex* 6, 342–353.
- Picard, N., Strick, P.L., 2001. Imaging the premotor areas. *Curr. Opin. Neurobiol.* 11, 663–672.
- Piekema, C., Kessels, R.P.C., Mars, R.B., Petersson, K.M., Fernandez, G., 2006. The right hippocampus participates in short-term memory maintenance of object–location associations. *NeuroImage* 33, 374–382.
- Prablanc, C., Martin, O., 1992. Automatic control during hand reaching at undetected two-dimensional target displacements. *J. Neurophysiol.* 67 (2), 455–469.
- Prevosto, V., Graf, W., Ugolini, G., 2010. Cerebellar inputs to intraparietal cortex areas LIP and MIP: functional frameworks for adaptive control of eye movements, reaching, and arm/eye/head movement coordination. *Cereb. Cortex* 20, 214–228.
- Ranganath, C., D'Esposito, M., 2001. Medial temporal lobe activity associated with active maintenance of novel information. *Neuron* 31, 865–873.
- Redding, G.M., Wallace, B., 2002. Strategic calibration and spatial alignment: a model from prism adaptation. *J. Mot. Behav.* 34 (2), 126–138.
- Rolls, E.T., 1991. Functions of the primate hippocampus in spatial processing and memory. In: Paillard, J. (Ed.), *Brain and Space*. Oxford University Press, Oxford, pp. 353–376.
- Rolls, E.T., 1999. Spatial view cells and the representation of place in the primate hippocampus. *Hippocampus* 9, 467–480.
- Sainburg, R.L., 2002. Evidence for a dynamic-dominance hypothesis of handedness. *Exp. Brain Res.* 142, 241–258.
- Sainburg, R.L., Kalakanis, D., 2000. Differences in control of limb dynamics during dominant and nondominant arm reaching. *J. Neurophysiol.* 83, 2661–2675.
- Salowitz, N.M.G., Zimelman, J., Simo, L., Suminski, A.J., Scheidt, R.A., 2010. Behavioral regression in functional magnetic resonance image analysis of sensory-motor learning. *Soc. Neurosci (San Diego CA)*.
- Sanes, J.N., 2003. Neocortical mechanisms in motor learning. *Curr. Opin. Neurobiol.* 13, 225–231.
- Sanger, T.D., 1989. Optimal unsupervised learning in a single-layer linear feedback neural network. *Neural Netw.* 2, 459–473.
- Scheidt, R.A., Stoeckmann, T., 2007. Reach adaptation and final position control amid environmental uncertainty following stroke. *J. Neurophysiol.* 97, 2824–2836.
- Scheidt, R.A., Conditt, M.A., Reinkensmeyer, D.J., Mussa-Ivaldi, F.A., 2000. Persistence of motor adaptation during constrained, multi-joint, arm movements. *J. Neurophysiol.* 84, 853–862.
- Scheidt, R.A., Dingwell, J.B., Mussa-Ivaldi, F.A., 2001. Learning to move amid uncertainty. *J. Neurophysiol.* 86, 971–985.
- Schultz, W., Apicella, P., Ljungberg, T., 1993. Conditioned stimuli during successive steps of learning a delayed response task. *J. Neurosci.* 13 (3), 900–913.
- Schultz, W., Apicella, P., Romo, R., Scarnati, E., 1995. Context-dependent activity in primate striatum reflecting past and future behavioral events. In: Houk, James C., Davis, Joel L., Beiser, David G. (Eds.), *Models of Information Processing in the Basal Ganglia*. MIT Press, Cambridge, Massachusetts.
- Schultz, W., Dayan, P., Read-Montague, P., 1997. A neural substrate of prediction and reward. *Science* 275, 1593–1599.
- Schultz, W., Tremblay, L., Hollerman, J.R., 2000. Reward processing in primate orbitofrontal cortex and basal ganglia. *Cereb. Cortex* 10, 272–283.
- Scott, S.H., 2004. Optimal feedback control and the neural basis of volitional motor control. *Nat. Rev. Neurosci.* 5, 534–546.
- Seidler, R.D., Noll, D.C., Thiers, G., 2004. Feedforward and feedback processes in motor control. *NeuroImage* 22, 1775–1783.
- Seidler, R.D., Noll, D.C., Chintalapati, P., 2006. Bilateral basal ganglia activation associated with sensorimotor adaptation. *Exp. Brain Res.* 175, 544–555.
- Selemon, L.D., Goldman-Rakic, P.S., 1985. Longitudinal topography and interdigitation of corticostriatal projections in the Rhesus monkey. *J. Neurosci.* 5 (3), 776–794.
- Selemon, L.D., Goldman-Rakic, P.S., 1988. Common cortical and subcortical targets of the dorsolateral prefrontal and posterior parietal cortices in the rhesus monkey: evidence for a distributed neural network subserving spatially guided behavior. *J. Neurosci.* 8 (11), 4049–4068.
- Serrien, D.J., Wiesendanger, M., 1999. Grip-load force coordination in cerebellar patients. *Exp. Brain Res.* 128, 76–80.
- Shadmehr, R., Holcomb, H.H., 1997. Neural correlates of motor memory consolidation. *Science* 277, 821–825.
- Shadmehr, R., Krakauer, J.W., 2008. A computational neuroanatomy for motor control. *Exp. Brain Res.* 185, 359–381.
- Shadmehr, R., Mussa-Ivaldi, F.A., 1994. Adaptive representation of dynamics during learning of a motor task. *J. Neurosci.* 14, 3208–3224.
- Singer, T., Critchley, H.D., Preusschoff, K., 2009. A common role of insula in felings, empathy and uncertainty. *Trends Cogn. Sci.* 13 (8), 334–340.
- Smith, M.A., Ghazizadeh, A., Shadmehr, R., 2006. Interacting adaptive processes with different timescales underlie short-term motor learning. *PLoS Biol.* 4 (6), e179. doi:10.1371/journal.pbio.0040179.
- Spiegel, J., Schweighofer, N., Arbib, M.A., 2000. Cerebellar learning of accurate predictive control for fast-reaching movements. *Biol. Cybern.* 82, 321–333.

- Strick, P.L., 1978. Cerebellar involvement in volitional muscle responses to load changes. In: Desmedt, J.E. (Ed.), *Cerebral Motor Control in Man: Long Loop Mechanisms*. Karger, Basel, pp. 85–93.
- Suminski, A.J., Rao, S.M., Mosier, K.M., Scheidt, R.A., 2007a. Neural and electromyographic correlates of wrist posture control. *J. Neurophysiol.* 97, 1527–1545.
- Suminski, A.J., Zimelman, J.L., Scheidt, R.A., 2007b. Design and validation of a MR-compatible pneumatic manipulandum. *J. Neurosci. Methods* 163, 255–266.
- Sutherland, R.J., Whishaw, I.Q., Kolb, B., 1988. Contributions of cingulate cortex to two forms of spatial learning and memory. *J. Neurosci.* 8 (6), 1863–1872.
- Taira, M., Mine, S., Georgopoulos, A.P., Murata, A., Sakata, H., 1990. Parietal cortex neurons of the monkey related to the visual guidance of hand movement. *Exp. Brain Res.* 83, 29–36.
- Takahashi, C.D., Scheidt, R.A., Reinkensmeyer, D.J., 2001. Impedance control and internal model formation when reaching in a randomly varying dynamical environment. *J. Neurophysiol.* 86, 1047–1051.
- Talairach, J., Tournoux, P., 1988. *Co-Planar Stereotaxic Atlas of the Human Brain*. Thieme, Stuttgart.
- Thach, W.T., 1996. On the specific role of the cerebellum in motor learning and cognition: clues from PET activation and lesion studies in humans. *Behav. Brain Sci.* 19, 411–431.
- Thoroughman, K.A., Shadmehr, R., 1999. Electromyographic correlates of learning an internal model of reaching movements. *J. Neurophysiol.* 19 (19), 8573–8588.
- Todorov, E., Jordan, M.I., 2002. Optimal feedback control as a theory of motor coordination. *Nat. Neurosci.* 5 (11), 1226–1235.
- Toni, L., Schluter, N.D., Josephs, O., Friston, K., Passingham, R.E., 1999. Signal, set- and movement-related activity in the human brain: an event-related fMRI study. *Cereb. Cortex* 9, 34–49.
- Tseng, Y., Diedrichsen, J., Krakauer, J.W., Shadmehr, R., Bastian, A.J., 2007. Sensory prediction errors drive cerebellum-dependent adaptation of reaching. *J. Neurophysiol.* 98, 54–62.
- Tulving, E., 1987. Multiple memory systems and consciousness. *Hum. Neurobiol.* 6, 67–80.
- Tunik, E., Frey, S.H., Grafton, S.T., 2005. Virtual lesions of the anterior intraparietal area disrupt goal-dependent on-line adjustments of grasp. *Nat. Neurosci.* 4, 505–511.
- Tunik, E., Houk, J.C., Grafton, S.T., 2009. Basal ganglia contribution to the initiation of corrective submovements. *NeuroImage* 47, 1757–1766.
- Ullman, M.T., 2004. Contributions of memory circuits to language: the declarative/procedural model. *Cognition* 92, 231–270.
- Vaillancourt, D.E., Thulborn, K.R., Corcos, D.M., 2003. Neural basis for the processes that underlie visually guided and internally guided force control in humans. *J. Neurophysiol.* 90, 3330–3340.
- Vargha-Khadem, F., Gadian, D.G., Watkins, K.E., Connelly, A., Van Paesschen, W., Mishkin, M., 1997. Differential effects of early hippocampal pathology on episodic and semantic memory. *Science* 277, 376–380.
- von Holst, E., 1996. Relations between the central nervous system and the peripheral organs. In: Houck, Lynne D., Drickamer, Lee C. (Eds.), *Foundations of Animal Behavior: Classic Papers with Commentaries*. University of Chicago Press, Chicago, IL.
- von Holst, E., Mittelstaedt, H., 1950. Das Refferenzprinzip (Wechselwirkungen zwischen zentralnervensystem und peripherie). *Naturwissenschaften* 37 (20), 464–476.
- Ward, N.S., Swayne, O.B.C., Newton, J.M., 2008. Age-dependent changes in the neural correlates of force modulation: an fMRI study. *Neurobiol. Aging* 29 (9), 1434–1446.
- Wolpert, D.M., Kawato, M., 1998. Multiple paired forward and inverse models for motor control. *Neural Netw.* 11, 1317–1329.
- Wolpert, D.M., Ghahramani, Z., Jordan, M.I., 1995. An internal model for sensorimotor integration. *Science* 269, 1880–1882.
- Wolpert, D.M., Miall, R.C., Kawato, M., 1998. Internal models in the cerebellum. *Trends Cogn. Sci.* 2 (9), 338–347.
- Zimelman, J., Suminski, A., Rao, S., Scheidt, R., 2007. Predicting the Future: Neural Correlates of Internal Models in the Cerebellum and Anterior Cingulate. *Neural Cont. Movement Soc.*, Seville Spain.
- Zimelman, J.L., Suminski, A.J., Rao, S.M., Scheidt, R.A., 2008. Neural Correlates of Internal Models for Adapting Goal-directed Wrist Movements. *Abstr Am Phys Therapy Assn.*